Physics – Uspekhi **45** (4) 403 – 432 (2002)

REVIEWS OF TOPICAL PROBLEMS PACS numbers: 84.40.Be, 95.85.Bh, 96.40.Pg

Superhigh-energy cosmic ray detection using shower radioemission

A D Filonenko

DOI: 10.1070/PU2002v045n04ABEH000850

Contents

Abstract. It is argued that preconditions currently exist for more actively studying the possibility of detecting cosmic rays of superhigh energy (10^{21} – 10^{23} eV) by observing radio emission from a cascade shower. To illustrate this point, major results from the initial period of research (1961 – 1980) are briefly reviewed, problems unresolved at that time are pointed out, and subsequent advances that have stimulated further progress in this area are described.

1. Introduction

It is well known that the detection of high-energy cosmic rays, i.e. the determination of the initial particle energy, its motion direction, composition, etc., is made using traditional methods of registration of ionizing radiation based on the use of ionization and scintillation counters. In modern devices (detectors), which are designed to study particles with energies up to $W_0 > 10^{19}$ eV, the number of detectors can be quite large. Combined with power and signal communications, which are necessary for the detector to operate, such a system of counters is distributed over an area of 10 – 20 km^2. Such a detector does not directly register a primary particle striking its area; instead, it registers the electron-photon cascade (avalanche, shower) caused by this particle passing through the Earth's atmosphere. The cascade is several hundred meters across with a path inside the atmosphere (i.e. a longitudinal size) of several kilometers.

A D Filonenko East-Ukrainian National University,
Physics Department
Block Molodezhnyĭ 20A, 91034 Lugansk, Ukraine
Tel. (7-10 380 642) 46 41 54
E-mail: uni@vugu.lugansk.ua

Received 23 August 2000, revised 17 October 2001
Uspekhi Fizicheskikh Nauk **172** (2) 439 – 471 (2002)
Translated by K A Postnov; edited by S M Apenko and M I Zelnikov

Presently, cosmic ray science is a separate constituent part of high-energy astrophysics, this being entirely due to successes in developing registration methods of high-energy particles. At energies $W_0 > 10^{20}$ eV cosmic rays do not significantly alter their motion direction in galactic and intergalactic magnetic fields. This enables searches for the sources of these charged particles and the mechanisms for their acceleration to such high energies. However, the number of reliably registered events is insufficient for definitive conclusions to be made. Over the entire history of cosmic ray (CR) studies, only a dozen particles with energy $W_0 > 10^{20}$ eV have been detected.

Relatively recently, paper [1] reported the results of processing 36 events with energies exceeding 4×10^{19} eV. These data were obtained over a six-year period at the Akeno detector (Japan) with an area of about 100 km^2 Analysis indicated that with some probability these particles could come from three sites on the celestial sphere, two of which are associated with clusters of galaxies.

Paper [2] reported discovering a correlation between the direction of particles with energy $W_0 > 4 \times 10^{19}$ eV and pulsars located toward the entrance of the Local Arm of the Galaxy. The author of these observations [2] argues that pulsars could be the major source of particles with energies less than 4×10^{19} eV.

It is quite clear that these statistics are insufficient for definite conclusions to be drawn, and the working area of detectors should be increased to continue the studies. As is well known, the flux intensity of cosmic rays is

$$J_v(> W_0) = A \times W_0^{\gamma-1},$$

where $\gamma = 2.5-2.7$ is the energy-dependent spectral power law index. According to this expression, increasing the energy boundary by one order of magnitude (without changing the event rate) would require the detector area to increase by about 100 times. To assess the absolute values of the flux we note, for example, that at an energy $W_0 > 10^{20}$ eV the cosmic

ray flux intensity is such that on average one particle falls in an area of one km^2 per hundred years. At present, detectors with 1000 km^2 (the SHAL-1000 project [3, 4]) and 5000 km^2 (the Pierre Auger project [5]) areas have been designed and are under construction. The energies available for study with these detectors will be increased by about one order of magnitude.

Could we suppose that problems related to ultra-high energy cosmic rays will be resolved after that? The history of scientific research indicates that this would hardly be the case. However, it is impossible to imagine a traditional detector with a working area of $\approx 10^7$ km^2. Apparently, further energy extension of the experimental set-ups would be associated with elaboration of the CR registration method by observing radio emission from the electron–photon cascade in a condensed medium. The idea of radio detection was first put forward about 40 years ago [6] as follows. An electron–photon cascade in the Earth's atmosphere (a so-called broad air shower) is accompanied by Cherenkov coherent radiation emitted by excess electrons. The maximum of the radiation lies in the meter wavelength range. According to theoretical estimates, the radio emission intensity should be sufficient for reliable detection of the radiation field. The prospect for the radio detection method has been related to the possibility of using only a few simple antennas instead of a large number of scintillation counters. This would allow one to easily enlarge the energy range without significant difficulties, which are due to the necessity of long communication lines, labor-intensive maintenance of the detector components, and, possibly, the complexity of the obtained data analysis.

However, subsequent testing studies of the radiative mechanism and the detector realization have not justified the idea of changing the traditional detection methods. There are several reasons for this:

(1) a low excess in the signal amplitude over the cosmic radio noise;

(2) a narrow emission diagram with an angular size of the order of several degrees. This fact has virtually excluded the possibility of using a few antennas over a large area;

(3) the proportional increase of the signal with the air shower energy predicted by theory has not been found. The largest discrepancy takes place at high shower energies.

We can add that the radiative mechanism suggested in [6, 7] has been doubted. Moreover, the experimentally detected excess by several orders of magnitude in the radiation intensity at low energies over theoretically predicted values appeared very surprising.

Not having the possibility to discuss these problems in more detail, we note the core point. Apparently, the idea of replacing the traditional detectors with new ones has not been fully understood. Ionization and scintillation detectors are known to measure particle energies perfectly well up to about 10^{19} eV. Much more attention should probably be given to radio emission at moderate and low frequencies (0.1–1 MHz).

Classical electrodynamics does not allow the formation of narrow-beamed radiation if its wavelength exceeds the source size. The broad emission diagram is one of the main conditions for the radio detection method of very high energy cosmic rays ($W_0 > 10^{20}$ eV) to be applied. It seems likely that this is why after the studies at meter wavelengths have nearly ceased, the interest in low-frequency radio emission has significantly increased.

Unfortunately, the results of measurements obtained in most experiments cannot be considered to correspond to the studied task. Most frequently, this is due to the use of conductors of various forms as 'antennas' for the near zone ($R_0 \ll \lambda$). As a rule, they have been attached to the high-Ohmic input of the amplifier and often without any selection schemes. Evidently, in this case the signal amplitude at the amplifier output characterizes the potential of the Coulomb field of the excess air shower electrons and practically does not relate to the radiation field.

The radio emission from a broad air shower in the field of a thunderstorm cloud is one of the dominating mechanisms in the middle frequency range. However, due to field instability, this mechanism has not been invoked for cosmic ray detection. Of much more interest was the idea of the possibility of radio emission from the shower due to transition radiation of excess electrons. A charged particle with high energy ($\gamma \gg 1$) is known to radiate backwards in crossing the vacuum-conductor boundary. Here, practically all the energy is emitted within a narrow angle $\sim \gamma^{-1}$. However, this property can hardly be used for cosmic ray detection, first of all for technical reasons. It is easy to find (see, e.g., [8], p. 179) that some fraction of the emission also escapes in the boundary plane. Clearly, in this case the condition of quasi-coherent radiation from a broad air shower, caused by the collision of excess electrons with the Earth's surface, reads $\lambda > 2d$, where d is the shower cross section. The polarization of electromagnetic waves in this case will be vertical. If the shower energy is high, the radiation field, as calculations show, could be sufficient for a radio pulse to be detected.

Up to now, radio emission caused by excess electrons whose number is estimated [6] to be 10% of the maximum number of particles, i.e. $\sim 0.1N_0$, has been considered. The author of the present paper argues, based on calculations, that there exists a more efficient mechanism for radio emission from the shower related to transition radiation [9]. It is known that the motion of the shower disk in the Earth's magnetic field causes its polarization. The calculation indicates that, due to this mechanism, the centers of oppositely charged disks are located at a distance of 50 m from each other. With an rms shower radius of 70–100 m, the efficiency of the transition radiation mechanism from the electric dipole produced in this way is almost an order of magnitude higher than from the excessive electrons. This fact should certainly stimulate intensification of experimental studies of this phenomenon.

However, most appropriate mechanism for detecting of very high-energy cosmic rays is likely to be radio emission due to bremsstrahlung of δ-electrons of the shower. The authors [10–12] performed detailed calculations of the radiation field associated with the current of δ-electrons in the far zone and found that its efficiency can best be exploited for a shower in condensed media. The radiation there will be quasi-coherent. For the considered radiation mechanism due to the δ-electron current, this means that there is always a frequency range $0 < \nu < \nu_0$ where phases of electromagnetic waves from all sources (i.e. δ-electrons) differ by less than π. In this case they provide a positive contribution to the first half-period of the oscillatory contour of the radio detector, provided that its tuning frequency is $\lambda > 2L$. In other words, the quasi-coherent emission (radio receiving) is realized when the length of waves under study λ is at least two times as long as the shower length L.

Estimates show that near the Earth the strength of the field induced by the electron–photon cascade from a particle with energy $W_0 > 10^{23}$ eV on the lunar surface takes the value $\sim 0.5\ \mu V\ m^{-1}\ MHz^{-1}$ [13–15]. The longitudinal size of the cascade on the Moon is about 5–10 m (here we do not yet discuss the possible action of the Landau–Pomeranchuk–Migdal effect (LPM)). This corresponds to the coherent radiation active spectral bandwidth (i.e. when $\lambda > 2L$) from about 25 to 50 MHz. To register this signal, the UTR-2 telescope (Kharkov) is quite suitable. The radio signal amplitude excess over the cosmic radio noise is here about two to three orders of magnitude [14].

Carrying out such an experiment would not require the investment of significant funds. The information obtained from such an experiment is not limited to the registration of a primary particle but, as we shall show below, proves to be much richer. But most important is that in the case of a positive result from the experiment, the prospect of launching a space cosmic ray radio detector into lunar orbit opens up; here the energy range accessible for registration increases up to 10^{21}–10^{23} eV.

2. Mechanisms of radio emission from air showers

2.1 Coherent Cherenkov radiation

The idea of using the radio emissions accompanying an air shower for cosmic ray detection was recognized after the publication of paper [6], in which the author theoretically estimated the value of the excess negative charge of an electron–photon shower in a gaseous or condensed medium. The excess of electrons, according to [6], is a consequence of annihilation of the shower positrons and of Compton and δ-electrons appearing in the shower. The author of [6] argues that the excess of electrons with a mean energy of $\sim 10^8$ eV can reach 10% of the number of shower particles. If this number is large, the coherent emission of the excess negative charge can have substantial intensity.

Let us consider this process in more detail. First let us recall the general picture of the development of a broad air shower. The primary particle of very high energy (in most cases — a proton, less often — a heavier nucleus), by penetrating into the Earth's atmosphere, induces a chain of nuclear interactions yielding protons, neutrons and π-mesons, which, in turn, provoke new nuclear interactions. These particles form a narrow beam, called the shower trunk. At sea level, the trunk size does not exceed several meters.

In each nuclear interaction, a certain fraction of the energy is spent to form neutral π-mesons, which rapidly decay into high-energy photons. These photons, which appear inside the shower trunk, initiate electron–photon cascades (avalanches), which generate a large quantity of positrons and electrons. Due to multiple scattering in the atmosphere, these shower particles deviate off the trunk. Such scattering represents a gradual accumulation of a large number of small-angle deviations caused by the field of atomic nuclei. During their movement in the atmosphere, electrons and positrons come off the trunk by several hundred meters. At the shower's peak, the vast majority of these particles have an energy of 10^8 eV and their velocity is above that of electromagnetic waves in the atmosphere. So such a swarm of particles, where the number of electrons and positrons is as high as 95–98% of the total number, has the shape of a nearly flat disk 100 m in radius. About half of all the particles are found over the area of such a disk.

Positrons and electrons are created in equal numbers. However, by colliding with atomic electrons of the ambient medium, positrons annihilate, and the shower proves not to be neutral as a whole, since it contains a substantial number of excess electrons. In addition, the formation of Compton and δ-electrons also increases the number of excess electrons in the shower. δ-electrons are produced in collisions of shower particles with atoms of the medium inside which the shower propagates, i.e. are the result of ionization loss of high energy particles. The number of electrons thus formed with an energy above 1 keV is several orders of magnitude higher than the number of primary shower electrons, and, as estimates show (see Section 2.5), the radio emission intensity, caused by their braking, can be very high in a certain radio frequency range.

As is well known, the system of $n(t)$ particles, each of which for some probabilistic reasons (for example, as in radioactive decay) transits into another state (i.e. leaves the system under consideration), is described by the kinetic equation

$$dn = -\lambda n\, dt, \tag{2.1.1}$$

and its solution

$$n = n_0 \exp(-\lambda t)$$

gives the number of particles that remain in the system until moment t, if at $t = 0$ the system comprises n_0 particles. It is also known that the value of λ is numerically equal to the probability of a particle leaving (decay) the system, and the inverse value $\tau = 1/\lambda$ is equal to the time it takes for the particle number in the system to change by e times. If in this system there is also some mechanism to create the same particles, balance (2.1.1) must be written in the form

$$dn = \Phi(t)\, dt - \lambda n\, dt, \tag{2.1.2}$$

where $\Phi(t)$ is numerically equal to the number of particles produced per unit time at each moment.

The electron–photon avalanche at an arbitrary moment of time consists of $n_- = n_-(t)$ electrons and $n_+ = n_+(t)$ positrons. Each of these particles was produced by the same mechanism, which is described by some function $\Phi(t)$. The lifetime of positrons τ_+ and electrons τ_- is the time interval between the moment of the charged particle birth and the moment the energy is spent to form a γ-quantum (i.e. the moment of leaving the system). The rate of such particles leaving the avalanche could be equal for both species, provided no other annihilation channels exist for positrons. In contrast to electrons, positrons can annihilate in collisions with atomic electrons of the medium inside which the avalanche propagates. So the probability of particles leaving the avalanche can be related as

$$\frac{1}{\tau_+} = \frac{1}{\tau_-} + \frac{1}{\tau_a}, \tag{2.1.3}$$

where $1/\tau_a$ is the positron annihilation probability. Then Eqn (2.1.2) for two independent components of the system

consisting of electrons and positrons takes the form

$$\dot{n}_- = \Phi(t) - \frac{n_-}{\tau_-} + \dot{n}_{\delta,k}\,, \quad \dot{n}_+ = \Phi(t) - \frac{n_+}{\tau_+}\,, \tag{2.1.4}$$

where $\dot{n}_{\delta,k}$ is the number of Compton and δ-electrons of energy $\sim 10^8$ eV produced by the shower particles and quanta per unit time. In what follows, the author of [6] neglects this contribution because of the low efficiency of this mechanism in increasing the number of excess electrons.

After making the subtraction in Eqn (2.1.4), we get the equation for the particle excess $v = n_- - n_+$:

$$\dot{v} + \frac{v}{\tau_-} = \frac{n_+}{\tau_a} + \dot{n}_{\delta,k} \approx \frac{n_+}{\tau_a}\,. \tag{2.1.5}$$

Considering the above, it is natural to suppose that the right-hand-side of Eqn (2.1.5) depends exponentially on time, i.e. $n_+/\tau_a \approx A\exp(t/T_+)$, where T_+ is the characteristic growth time of the number of annihilating positrons. Then the solution to Eqn (2.1.5) will be

$$v \approx C^{-t/\tau_-} + \frac{A\exp(t/T_+)}{1/T_+ + 1/\tau_-} \approx \frac{n_+}{\tau_a(1/T_+ + 1/\tau_-)}$$

$$\text{at} \quad t \gg \tau_-\,.$$

It is clear from general considerations that the characteristic growth time T_+ of the number of annihilating positrons is proportional to τ_-, and then we can write approximately $v \sim n_+\tau/\tau_a$. The radiation length unit is the path the electron takes before its energy, mostly spent in the form of radiation, decreases by e times, so $\tau \approx l_{rad}/c$. According to the definition of the effective interaction cross section, the probability is $1/\tau_a \approx N_e\sigma_a c$, where the annihilation cross section [16] is

$$\sigma_a \approx \pi r_0^2\,\frac{mc^2}{E_+}\,\ln\frac{2E_+}{mc^2}\,.$$

It is known [17] that the radiation length unit is expressed as $l_{rad} = 137/4ZN_e r_0^2\,\ln(183/Z^{1/3})$. So we shall have the relation

$$\frac{\tau}{\tau_a} \approx \frac{137}{4Z}\,\frac{mc^2}{E_+}\,\frac{\ln(2E_+/mc^2)}{\ln(183Z^{1/3})}\,, \tag{2.1.6}$$

which is independent of the medium density and depends only on its particle's atomic number and energy. It is easy to confirm that for $Z = 10$ with a mean particle energy at the shower maximum of $E \approx 10^8$ eV, the ratio (2.1.6) is approximately 0.1. Let us find the value of the e.m.f. on terminals of a half-wavelength dipole as induced by a typical shower with energy $W_0 = 10^{17}$ eV. According to [6], the power radiated by the moving charges is $P = J_\omega\,\Delta\omega(Le^2c^2v^2\sin^2\alpha/4\pi\varepsilon_0\tau c^2)\,\omega\Delta\omega \approx 0.3\times10^{-6}$ W for $v = 0.1N_0 = 10^7$ and $\Delta\omega \approx 0.1\omega \approx 2\times10^7\ \text{s}^{-1}$ ($\lambda = 10$ m). For particles with a Lorentz-factor $\gamma \sim 200$ the Cherenkov angle $\alpha = 0.024$ (see Section 2.2) and the coherent length $L \sim 1$ km. A shower of such an energy reaches a maximum at an altitude of ~ 3 km. So the diameter of the region at the Earth's surface irradiated by the shower is $d = 150$ m. If a half-wave dipole serves as an antenna, its effective area $A = D_0\lambda^2/4\pi \approx 13\ \text{m}^2$, where $D_0 = 1.64$ is the maximum value of the directivity factor, and the power incident on this area is $P_1 = 4AP/\pi d^2 = 2\times10^{-10}$ W. The signal amplitude on the antenna terminals is $U_s = \sqrt{P_1 R} \approx 120$ μV. It is interesting to compare the energy fluxes related to the unit frequency from the shower and the celestial sphere (cosmic radio noise). For the shower this is $4P/\pi d^2\Delta v = 500\times10^{-20}\ \text{W m}^{-2}\ \text{Hz}^{-1}$. The corresponding value of the cosmic radio noise is [18]

$$J_v = 3\times10^{-40}Tv^2\ \text{W (m}^2\ \text{Hz sr)}^{-1}$$

$$\approx 2\times10^{-20}\ \text{W (m}^2\ \text{Hz sr)}^{-1}\,,$$

where $T \sim 10^4$ K is the effective temperature of the celestial sphere at the 30 MHz frequency. This means that the signal is about 16 times higher than the noise.

At radio frequencies, the non-compensated charge in the shower can exceed the intensity of Cherenkov, bremsstrahlung, and other radiation by orders of magnitude. This is related to the fact that at these wavelengths the radiation intensity is proportional to the frequency square v^2 and the number of particles in the shower.

The size of the shower extension region is determined by the medium density. In the air, the shower cross section is about 100 m, and the wavelengths produced by this radio emission mechanism are several meters. In dense media the coherent radio emission lies within the wavelength range 1 – 100 cm, and then the Cherenkov radiation intensity is the most significant.

This fact can be used for the registration of cosmic rays of high penetration capability, for example, μ-mesons. Extensive underground zones were experimentally found to exist, within which radio waves can propagate over appreciable distances. In addition, the Earth's surface layer is known to fully screen the interior zones from external electromagnetic noise. So such underground regions are very convenient for observing the radio pulses that accompany cascade showers generated by deeply penetrating particles.

The results of studies of radio emission from air showers before publication [6] appeared, had left almost no hope for practical application of the radio detection method. This had been connected mostly to the absence of grounds for the consideration of a coherent radio emission model. So paper [6] from my point of view became a strong stimulating factor. Moreover, it pointed to other possible coherent emission mechanisms: that due to the shower polarization in the Earth's magnetic field and that of transition radio emission by the excess electrons crossing the air – soil boundary. In addition, attention was first drawn to the possibility of using the lunar surface as a working area of the detector. However, it took another several years to recognize these conclusions. And only in 1965 did publications appear with the results of theoretical and experimental studies.

A numerical estimates of the Cherenkov radio emission from a broad air shower were obtained in paper [19], which was in fact the continuation of paper [6]. In these calculations, the author used a model air shower, in which excess electrons were uniformly distributed across a shower disk of effective radius of about 30 m, which corresponds to the emission frequency maximum near $v = 50$ MHz. The disk thickness is much smaller than its diameter, so in moving inside the atmosphere with a velocity exceeding that of the electromagnetic wave propagation, the excess shower electrons induce coherent Cherenkov radiation. According to [9], the angular diameter of the principal maximum of the spatial emission diagram is approximately equal to 3×10^{-2} sr, which corresponds to an irradiated area on the Earth's surface of around $10^5\ \text{m}^2$. For a shower of $N_0 = 10^{10}$ particles and the frequency interval $\Delta v = 10^{-2}\,v$, the radio emission pulse power is $\sim 10^{-3}$ W, as estimated in [19].

2.2 Geomagnetic radiation mechanisms

The replenishment of particles in the electron–photon avalanche occurs in a time interval approximately equal to the ratio of the radiation length unit to the velocity $c \approx 3 \times 10^8$ m s^{-1}. Since for the normal atmosphere $t_0 \approx 300$ m, the mean 'life-time' of a particle, i.e. the time it takes for its energy to decrease e times, is $\tau = t_0/c = 10^{-6}$ s. In addition to the action of neutral atoms in the atmosphere, which leads to particle scattering and the formation of a broad air shower, the Earth's magnetic field affects charged particles of the air shower. This causes a directional motion, superimposed on the charge-independent transversal motion, to appear perpendicular to both the shower axis and the magnetic field, with electrons and positrons moving in opposite directions. This phenomenon formally looks like the behavior of free electrons in a conductor with a constant potential difference applied. In both cases such a directional motion of particles represents an electric current with a value determined by the charge passing through the conditional cross section area.

This transverse current in the shower can be considered as a cause of the polarization of the entirely neutral disk. Moving in a magnetic field, the positron disk gets separated from the electron disk in the opposite direction, thereby forming an electric dipole directed in the transverse current direction. Inside the disk motion interval where the number of particles is close to the maximum, a dynamical quasi-equilibrium can be assumed in the transverse direction when the number of particles created within the trunk is equal to the number leaving the shower. So broad air showers can be thought of as a moving quasi-static dipole in which the transverse current sustains the dipole moment.

It is known that if the angle between the magnetic field direction **H** and the shower axis is β, the transverse acceleration of the charged particles moving in the magnetic field with a velocity close to that of light in vacuum is $eH \sin\beta/\gamma m_0$ (everywhere in this section we use the CGS system), where m_0 is the rest mass of the particle, and γ is the Lorentz-factor, which is about 200 for the shower electrons (and positrons). The transverse shift of charged particles of one sign $\Delta = (1/\gamma m_0)\, eH\tau^2 \sin\beta$ and the dipole moment induced by displacement of the disks $M = (1/\gamma m_0) e^2 N H \tau^2 \sin\beta$, where Ne is the charge of one of the disks.

Thus, in the model of the geomagnetic radio emission mechanism [7], the propagation of a broad air shower is accompanied by the following processes leading to radiation:

(a) the appearance of an excess charge of $Q = 0.1q = 0.1Ne$;

(b) the transverse motion of a quasi-static dipole with a velocity exceeding that of electromagnetic waves in the Earth's atmosphere;

(c) the same motion of the transverse current sustaining disk polarization.

In paper [5] radiation intensities due to these mechanisms are compared. The solution of each of these tasks is found using the Maxwell equations for potentials (see, e.g., [20])

$$\Delta\varphi(\mathbf{r}, t) - \frac{\varepsilon}{c^2}\,\frac{\partial^2\varphi}{\partial t^2} = -\frac{4\pi}{c}\,\rho(\mathbf{r}, t)\,, \qquad (2.2.1)$$

where $\rho(\mathbf{r}, t)$ is the volume charge density, ε the dielectric permeability and $c = 3 \times 10^{10}$ cm s^{-1} is the velocity of electromagnetic waves in vacuum. Let the Ox axis be directed along the shower axis and the electric dipole moment along the Oz axis. To simplify the physical model, we assume the shower disk to be an infinitely thin plane, over which excessive charges are distributed with density $\sigma = \sigma(y, z)$. Using the δ-function properties, the volume charge density can be written in the form

$$\rho(x, y, z, t) = \sigma(y, z)\,\delta(x - ut)\,,$$

where u is the longitudinal disk velocity.

Eqn (2.2.1) can be simplified by eliminating the time and considering the equation for amplitudes of the Fourier expansion for these values:

$$\delta(x - ut) = \frac{1}{2\pi}\int_{-\infty}^{\infty} \exp\left[\mathrm{i}k(x - ut)\right] \mathrm{d}k\,, \qquad (2.2.2)$$

$$\varphi(x, y, z, t) = \int_{-\infty}^{\infty} \Phi(k, y, z) \exp\left[\mathrm{i}k(x - ut)\right] \mathrm{d}k\,, \qquad (2.2.3)$$

where $k = 2\pi f/u$ is the wave number.

Substituting (2.2.2) and (2.2.3) into (2.2.1) yields

$$\frac{\partial^2\Phi}{\partial y^2} + \frac{\partial^2\Phi}{\partial z^2} + k^2 \tan^2\alpha\Phi(y, z, k) = -2\sigma(y, z)\,, \qquad (2.2.4)$$

if the velocity c' of the electromagnetic waves in the atmosphere with refraction index n is equal to c/n and is related to the Cherenkov angle through the expression $\cos\alpha = c'/u$. In addition, we should bear in mind that for this substitution Eqn (2.2.1) turns into identity.

For further simplification of the model, the authors [7] assumed that the excessive shower charge $Q = 0.1Ne$ is uniformly distributed over an infinitely thin ring of radius a. In this case, we can again use the δ-function properties to express the surface charge density $\sigma(y, z)$ in Eqn (2.2.4). In the cylindrical frame, the correctly chosen expression for $\sigma(r)$ must satisfy the equality:

$$Q = \int_0^{2\pi} \mathrm{d}\varphi \int_0^{\infty} C\,\delta(r - a)\, r\,\mathrm{d}r\,,$$

hence $C = Q/2\pi a$ and $\sigma(r) = (Q/2\pi a)\,\delta(r - a)$. Eqn (2.2.4) in the cylindrical frame then takes the form

$$\frac{\mathrm{d}^2\Phi}{\mathrm{d}r^2} + \frac{1}{r}\,\frac{\mathrm{d}\Phi}{\mathrm{d}r} + k^2 \tan^2\alpha\Phi(k, r) = -\frac{Q}{\pi a}\,\delta(r - a)\,. \qquad (2.2.5)$$

The solution of this equation in the region $r > a$ is the function

$$\Phi_{\mathrm{s}} = \frac{1}{2}\,\mathrm{i}QJ_0(k\alpha a)\, H_0^{(1)}(k\alpha r)\,, \qquad (2.2.6)$$

and the field strength radial component for the unit wave vector interval is

$$E_{\mathrm{s}} = -\frac{\mathrm{d}\Phi_{\mathrm{s}}}{\mathrm{d}r} = -\frac{1}{2}\,\mathrm{i}k\alpha QJ_0(k\alpha a)\, H_0^{(1)\prime}(k\alpha r)\,, \qquad (2.2.7)$$

where J_0 is the zero-order Bessel function of the first kind and $H_0^{(1)}$ is the zero-order first Hanckel function. For $r < a$ the waves are standing.

The field induced by the quasi-static dipole is found as a superposition of fields (2.2.6) produced by disks of charge $q = Ne$. As the distance between the disks Δ is approximately

10 m, i.e. much smaller than the system size, the resulting field potential is determined by the expression

$$\Phi_{\rm p}(r,\theta) = \Phi_{\rm s}(r - \Delta\cos\theta) - \Phi_{\rm s}(r) = -\frac{1}{2}\,{\rm i}q\Delta\cos\theta\, k\alpha\, J_0(k\alpha a)\, H_0^{(1)\prime}(k\alpha r)\,, \qquad (2.2.8)$$

where θ is the angle between the Oz axis and the line of sight. In this case the field strength has both radial and azimuthal components:

$$E_{\rm p}^{(r)} = \frac{{\rm i}M\cos\theta}{2}\, k^2\alpha^2 J_0(k\alpha a)\, H_0^{(1)\prime\prime}(k\alpha r) \quad (r > a)\,,$$

$$E_{\rm p}^{(\theta)} = -\frac{{\rm i}M\sin\theta}{2r}\, k\alpha\, J_0(k\alpha a)\, H_0^{(1)\prime}(k\alpha r) \quad (r > a)\,, \qquad (2.2.9)$$

where $M = q\Delta$.

The field induced by the charged particle motion is described by Maxwell's equation for the vector potential:

$$\mathbf{A}(\mathbf{r},t) - \frac{\varepsilon}{c^2}\,\frac{\partial^2\mathbf{A}}{\partial t^2} = -\frac{4\pi}{c}\,\mathbf{j}(\mathbf{r})\,, \qquad (2.2.10)$$

where $\mathbf{A}$ is the field vector potential, $\mathbf{j}$ is the current density, $c = 3\times10^{10}$ cm s^{-1} is the electromagnetic wave speed in vacuum, and ε is the dielectric permeability of the medium. The current density $\mathbf{j}$ is produced by all elements of the ring of charge $q = Ne$. The current density caused by a point charge $\mathrm{d}q$ moving with velocity $\mathbf{v}$ is given by

$$\mathrm{d}\mathbf{j} = \mathrm{d}q\,\mathbf{v}\delta(\mathbf{r} - \mathbf{r}_0)\,,$$

where $\mathbf{r}_0 = \mathbf{r}_0(t)$ is the trajectory of motion, and $\mathbf{r}$ is the radius-vector of an arbitrary point of space. The δ-function implies the equality

$$\delta(\mathbf{r} - \mathbf{r}_0) = \delta(x - x_0)\,\delta(y - y_0)\,\delta(z - z_0)\,,$$

so in Maxwell's equation for the vector potential $\mathbf{A}(\mathbf{r},t)$ induced by the motion of, for example, the shower negative charge q_- in the terrestrial magnetic field, the current density can be written in the form

$$\mathbf{j}_- = q_-(\mathbf{u} + \mathbf{v})\,\delta(\mathbf{r} - \mathbf{r}_0)\,,$$

where $\mathbf{u}$ is the longitudinal velocity and $\mathbf{v}$ is the transverse velocity.

Within the framework of the model considered by the authors of [7], $|\mathbf{v}| \ll |\mathbf{u}|$. However, electrons and positrons in the longitudinal direction move in one direction, and this component of the current is zero (in the model of radiation the disks are assumed to have the same but opposite sign charges). In the transverse direction, electrons and positrons move oppositely and the total current will be twice as much as from the particles of one sign. In the cylindrical frame, each charged element of one of the rings $\mathrm{d}q = q\,\mathrm{d}(\theta a)/2\pi a$, where θ is the azimuthal angle, produces the charge density

$$\mathrm{d}\mathbf{j} = \frac{q\mathbf{v}}{2\pi a}\,\mathrm{d}(\theta a)\,\delta(r - a)\,\delta(x - ut)\,\delta(\theta a)\,.$$

After summing over all elements of the ring, we get

$$\mathbf{j} = \frac{q\mathbf{v}}{2\pi a}\,\delta(r - a)\,\delta(x - ut)\,. \qquad (2.2.11)$$

This expression shows that the current density is non-zero only inside a narrow interval $\Delta \to 0$, and the charge direction is along the Oz-axis. At the same time, the particles move along the shower axis with velocity $\mathbf{u}$. So the vector potential has one component and Eqn (2.2.10) with the right-hand-side (2.2.11) is solved in a way similar to the above case for the potential $\Phi(y,z,k)$. The vector potential in the region $r > a$ reads

$$A = \frac{{\rm i}q\Delta}{2c\tau}\, J_0(k\alpha a)\, H_0^{(1)}(k\alpha r)$$

and the field strength radial component is

$$E_{\rm c}^{(r)} = -\frac{kq\Delta}{2c\tau}\cos\theta\, J_0(k\alpha a)\, H_0^{(1)}(k\alpha r)\,. \qquad (2.2.12)$$

According to Eqns (2.2.12), (2.2.9) and (2.2.7) for the field strength due to the corresponding radio emission mechanisms (the dipole current, quasi-static dipole, and excessive shower charge), the ratio of strengths for the first pair is

$$\left|\frac{E_{\rm c}^{(r)}}{E_{\rm p}^{(r)}}\right| = \frac{1}{kc\tau\alpha^2} = 11:2\,,$$

if $k = 10^{-2}$ cm^{-1}, $\tau = 10^{-6}$ s, $\alpha = 0.024$, and $c = 3\times10^{10}$ cm s^{-1}. For the last two mechanisms

$$\frac{E_{\rm p}^{(r)}}{E_{\rm s}^{(r)}} = \left(\frac{Q}{q}\right) : \left(\frac{\Delta}{r}\right) = r\times10^{-4}\,,$$

if $Q/q = 0.1$, $\Delta = 10^3$ cm, and $\cos\theta \sim 1$. This means that the dipole moment will dominate when $r < 100$ m. The above estimates imply that for $r > a$ the dipole current emission mechanism is much more efficient than others. The authors of [7] also carried out a comparative analysis of the efficiency of the mechanisms for $r < a$. They found that the mechanism corresponding to the dipole current dominates in this region as well, except for a small zone in the center with a radius of about 17 m.

The energy emitted by the shower per unit area per unit frequency range at the distance r from the observer is found according to Parceval's theorem:

$$\frac{\pi}{c}\,EE^* = \frac{\pi k^2\Delta^2q^2}{4c^3\tau^2}\, J_0^2(k\alpha a)\left|H_0^{(1)}(k\alpha r)\right|^2.$$

All the above estimates were made by the authors of [7] for a shower in which the number of particles is conserved during the motion, and the current density stays constant. To approach reality, the authors assumed that the shower current density changes with the depth as $j = j_0\exp(-\lambda x)$. For reasonable values $\lambda \ll 3\times10^{-6}$ cm^{-1}, the estimates do not change significantly.

2.3 Geoelectric radiation mechanisms

Radio emission can be generated by an accelerated motion in the electrostatic field of the Earth, whose intensity near the surface in fine weather is about 100 V m^{-1}, gradually decreasing to 1 V m^{-1} at 20 km altitude. The authors of [21–23] consider three cases that lead to radio emission from a broad air shower in the static field.

1. The transverse separation of the fast shower particles (with an energy of up to 10^8 eV) due to the field component perpendicular to the motion direction (i.e. only for inclined and horizontal showers). This case is like the effect of

geomagnetic shower charge separation [7]. The electric field initiates charge separation

$$\Delta_{\mathrm{TE}} = \frac{eE_T}{\gamma m_0}\,\tau^2\,,$$

where e is the electron charge, γ the Lorentz-factor, m_0 the electron rest mass, E_T the field component perpendicular to the shower motion direction, τ the time it takes for the particle to spend its energy, i.e. $\tau \approx 10^{-6}$ s at sea level, and c the speed of light. It is easy to find that the value of Δ_{TE} will be of the same order of magnitude as in the case of the magnetic charge separation if $E_T \sim H_T c$. For $H_T \sim 0.2$ E , E_T must be about 6 kV m^{-1}. So under normal conditions, the charge separation effect due to the geoelectric field must be insignificant.

2. The longitudinal separation of fast particles due to the field component E_{p} parallel to the shower propagation direction is characterized by the displacement $\Delta_{\mathrm{p}E}$, which has no analogue in case of magnetic field:

$$\Delta_{\mathrm{p}E} = \frac{eE_{\mathrm{p}}}{\gamma^3 m_0}\,\tau^2\,.$$

Ignoring the negative charge excess, the shower can be approximated by a set of electric dipoles with axes oriented along the geoelectric field E_{p}. It has the form of a disk 70 m in radius at sea level and ~ 2 m in thickness. For a wavelength range much in excess of the disk thickness, the Cherenkov radiation will be quasi-coherent. This effect, however, is negligible as $\Delta^2_{\mathrm{p}E} \ll \lambda^2$.

3. The motion of slow (ionization) electrons, i.e. those which are unable to ionize atoms of the air due to the energy deficit. After thermalization in elastic collisions they move along the external field direction and in a time $\sim 10^{-7}$ s are captured predominantly by oxygen molecules [23–25].

The acceleration of fast electrons in the transverse direction is proportional to γ^{-1}, and in the longitudinal direction to γ^{-3}. For fast particles of the shower $\gamma \approx 200$, so the generation of radiation in the former case is more efficient. However, to attain an efficiency comparable to that of the geomagnetic or Cherenkov mechanisms, the needed static field strength is evaluated by the authors of [22] to be about 6×10^3 V m^{-1}, which can take place only during unstable weather conditions. An analysis of the third case suggested the possibility of its providing an appreciable contribution to the emission for horizontal showers comparable to emission from excess electrons.

2.4 Radio emission due to ionization electrons in the atmospheric electricity field

Radio emission produced by acceleration of ionization electrons in the field of a thunderstorm cloud is considered in [24]. The author of [24] concludes that there is a possibility of a radio emission mechanism similar to the Cherenkov radiation when the source has a velocity much less than the speed of electromagnetic waves. The essence of the effect in this case is in the known beforehand 'program of turning-on' of emitters — ionization electrons. The emitters start operating by the arrival time of the disk shower whose velocity exceeds the field propagation speed in the medium. However, a detailed study indicates that this emission, in the author's opinion, does not principally differ from Cherenkov radiation.

To calculate the radiation field, paper [24] considers the current of ionization electrons modulated by the cascade function of the shower:

$$j = j_0 \exp\left[\frac{\eta\upsilon}{c'}\,(x - c't) - b|x|\right],$$

where $\eta\upsilon$ is some kinematic characteristic of the atmosphere weakly depending upon the drift velocity υ and the ratio E_{p}/p of the electrostatic field strength to the atmospheric pressure at a given altitude, c' is the propagation speed of the shower, and b is a constant characterizing the degree of modulation of the current as a function of the altitude.

To simplify calculations in this model, the cross section of the shower is assumed infinitely small. By applying the standard procedure of expanding the ionization electron current in Fourier components, the author of [24] found the spectral component of the radiation field strength. This paper has no room to illustrate the cumbersome formulas and expressions as derived in [24]. So we shall restrict ourselves to briefly considering the results. Table 1 lists the absolute values of the Poynting vectors for some frequencies.

Table 1.

E_{p}/p, (V m^{-1}) mm^{-1}	β	Poynting vector for frequencies			
		100 kHz	500 kHz	2.5 MHz	12.5 MHz
0.4×10^2	0.01	3.7×10^{-26}	8.9×10^{-25}	9.1×10^{-24}	5.7×10^{-25}
	0.10	3.4×10^{-26}	2.1×10^{-25}	1.8×10^{-26}	7.5×10^{-29}
4×10^2	0.01	3.4×10^{-23}	3.8×10^{-22}	4.4×10^{-22}	1.1×10^{-23}
	0.10	2.9×10^{-23}	8.8×10^{-23}	8.9×10^{-25}	1.5×10^{-27}

The radiation field strength caused by ionization electron acceleration can be quite substantial only in a geoelectric field of strength $\sim 10^6$ V m^{-1}. Such a conclusion was made in papers [23, 25] as well, where the estimates of the field in this mechanism were obtained in the spectral range 10 kHz–10 MHz. In paper [25], a comparative analysis was carried out of the calculated field strength and experimentally obtained values for the frequency range 100 kHz–6 MHz. Here the author comes to a conclusion that the spectral intensities of the geoelectric and geomagnetic [7] mechanisms are nearly equal at frequencies around 100 kHz.

This radio emission mechanism is connected to the experimentally detected phenomenon of an anomalously high radio pulse amplitude accompanying broad air showers. It is well established that under some conditions (depending on the state of the atmosphere), anomalously high radio emission is observed from an air shower produced by a primary particle with energy $W_0 \geqslant 10^{16}$ eV (see, for example, [26–28]). To date, no definite explanation of this phenomenon has been suggested. However, many attempts have been made to understand its nature. It is quite probable that such an anomaly is due to the increase in the atmospheric electricity field strength in unstable weather conditions.

In [26–27], the authors declined to explain the nature of the anomalous radio pulse by radiation of excess shower electrons and proposed that the observed phenomenon is a consequence of an electric break-down in the atmosphere along the ionization track formed by the shower disk propagation. However, simple estimates indicate that the electromagnetic field strength in this case is many orders of magnitude higher that the experimental values. For example, the electromagnetic pulse amplitude registered in [26] corre-

sponded to a field strength of ~ 0.05 V m^{-1} within the chosen frequency range, which is much smaller than the field strength induced by a lightning discharge even at a relatively remote distance.

The author of paper [29] also believes that the origin of the anomalous radio pulse is linked to the high field strength of the atmospheric electricity, but unlike [21, 22, 25, 26] assumes the intense radio emission to be due not to the longitudinal current of excess electrons, but the transverse current of ionization electrons in the thunderstorm cloud field. Moreover, it is also shown in [29] that the reason for the anomalously high intensity of emission can be connected to a sharp emission beam diagram for strongly inclined showers. Electrons and positrons of a broad air shower, having an energy of 10^8 eV, ultimately spend their energy on ionization or excitation of atmospheric atoms. It is known that the ionization of an atom requires an energy of about 30 eV on average.

After thermalization, an ionization electron drifts along the field for a time τ_a until it 'sticks' to a neutral oxygen molecule. The sticking time, i.e. the drifting time of the thermalized electron, is of the order of 10^{-7} s and naturally depends upon the concentration of neutral molecules [31]. Such electron motion is an elementary act of the anomalous radio emission of an air shower.

The possibility of the transverse electron drift in a thunderstorm cloud field has a fundamental significance. The point is that antennas registering radio emission have been located very close to the shower axis in the above experiments ($\sim 0.2-1$ km). It is also known that the spatial emission diagram of a charged particle passing a certain distance R_δ has a maximum in the plane perpendicular to the direction of motion $\mathbf{R}_\delta$, and a zero minimum along the movement. This conclusion holds inside the wavelength range $\lambda \gg R_\delta$ and for the time of motion $\omega\tau_a \leqslant 1$ (see [20, 30]).

In this case, the spectral component of the field (V m^{-1} Hz^{-1}) can be represented by the simple expression [10, 11, 20, 30]

$$E_1(\omega) = \frac{q\,\mathrm{i}\,\omega \exp(\mathrm{i}kR_0)R_\delta}{4\pi\,\varepsilon_0 c^2 R_0}\sin\alpha\,, \qquad (2.4.1)$$

where q is the particle charge, ω are the frequencies of the infinitely close harmonics, R_0 is the distance between the charge and the observer, R_δ is the length of the charged particle path until complete stop, α is the angle between the direction of the particle motion and the observer, $k = \omega/c$, $c = 3\times 10^8$ m s^{-1}, and $(4\pi\varepsilon_0)^{-1} = 9\times 10^9$ m F^{-1}.

As follows from Eqn (2.4.1.), no emission is radiated in the direction $\alpha = 0$. So for the observer located near the shower axis (this is important now), the most effective radiation mechanism is that connected to the transverse drift of electrons, i.e. for $\alpha = \pi/2$. In addition, the quantity of excess electrons, as calculations [6] indicate, does not exceed 10% of their total number. For example, for a shower with energy $W_0 = 10^{17}$ eV, the total number of electrons at the maximum N_0 is about 10^8, and the number of excess electrons is 10^7, correspondingly. The number of ionization electrons in this example is $10^{17}/30 \approx 3\times 10^{15}$, i.e. eight orders of magnitude higher than the excess electrons. So the radio emission due to ionization electrons can be much more efficient.

To evaluate the electromagnetic field strength caused by the transverse drift of ionization electrons, we consider the following idealized model for a broad air shower. The air shower consists of a set of N_0 charged particles (electrons and positrons) within the volume of a negligibly thin, wholly neutral disk of radius r_0 moving with a velocity close to the speed of light in vacuum ($\gamma \approx 200$). The active part of the path of this disk L is about several kilometers. Practically all the primary particle energy W_0 is spent on ionization and excitation of the molecules of the atmospheric air.

The maximum stage of the shower (i.e. when the particle number is close to N_0) occurs at an altitude of several kilometers. Clearly, electrons of ionized molecules, not the shower charged particles, are emitters in this model, which before the shower disk arrival were 'at rest'. After ionization of the molecules, thermalized electrons drift along the direction of the field.

In this case, for the observer located near the shower axis (see note above), the angle $\alpha \approx \pi/2$ if the electrostatic field is perpendicular to the shower axis (for example, a thunderstorm cloud field). The elementary emitters can be assumed to be practically immobile with respect to the disk, as its drift velocity is $v_d = qE_\perp/mv_m$ which even in a field $E_\perp = 10^5$ V m^{-1} is 2×10^5 m s^{-1}, i.e. three orders of magnitude less than the speed of light.

Let us assume further that the observer is inside the wave zone, so $\lambda \ll R_0$. For the given observation direction θ (the angle between the shower axis and R_0) we determine the frequency range $0 \leqslant \omega \leqslant \omega_0$ inside which the phase difference $\Delta\varphi$ of the electromagnetic waves reaching the observer from any point of the disk will not exceed π. In this case, to assess the field strength at the point of observation, the amplitudes of elementary harmonics (2.4.1) can be added arithmetically.

Figure 1 shows the position of the disk ($AB = d = 2r_0$) at the 'initial' moment. In time t it will be at position $A'B'$ with $AA' = BB' = vt$ and $AE = BF = ct$ being the path the wave travels over this time interval in the direction θ. At $t = 0$ the phase difference between the signals coming from points A and B is determined by the picture geometry only and is $d\sin\theta$. As the shower progresses and ionization of the air molecules proceeds, each of the electrons released from atoms becomes, over the period of time τ_a, an elementary source of electromagnetic waves with amplitude $E(\omega)$ determined by expression (2.4.1). For the arbitrary moment t, when the disk is at the position $A'B'$, the phase difference $\Delta\varphi$ will be maximal between the wave traveling from point B at the moment $t = 0$ and the wave traveling from point A' at the

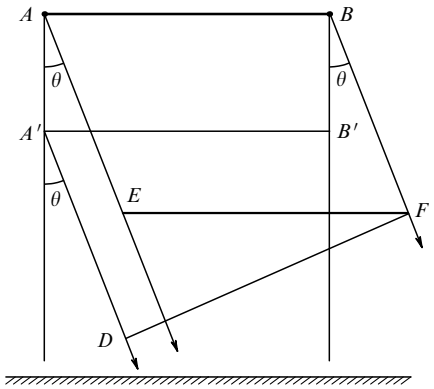

Figure 1. Determination of the phase difference at the point of observation: AB and $A'B'$ — the shower disk positions at different times, $A'D$ and AE — the radiation directions.

arbitrary moment t. As is seen from the figure,

$$\Delta\varphi = A'D\,\frac{2\pi}{\lambda} = (d\sin\theta + ct - vt\cos\theta)\,\frac{2\pi}{\lambda}\,.$$

The frequency interval $\Delta\omega = \omega_0$ is obtained by substituting $t = L/v$:

$$\Delta\omega = \frac{\pi c}{\beta\, d\sin\theta + L(1-\beta\cos\theta)}\,. \qquad (2.4.2)$$

Let us choose, for example, the angle $\theta = 10^\circ$. In this case it is easy to find that for an isotropic distribution of cosmic ray propagation in space, about 2% will have a direction such that an observer on the Earth will be inside a radiation cone with angle $2\theta = 20^\circ$. Substituting into Eqn (2.4.2) the characteristic values $L = 3\times10^3$ m, $\beta = 0.9998$ (for $\gamma = 50$), $d = 2r_0 = 200$ m, $c = 3\times10^8$ m s^{-1}, we get $\Delta\omega = 10^7$ s^{-1}. The free path for the thunderstorm cloud field of $E_\perp = 10^5$ V m^{-1} has a value of $R_\delta = qE_\perp\tau_a/mv_m = 6\times10^{-2}$ m, where $q = 1.6\times10^{-19}$ C, $\tau_a = 3\times10^{-7}$ s, $m = 0.9\times10^{-30}$ kg, $v_m = 0.8\times10^{11}$ s^{-1} is the number of collisions per unit time with neutral atoms (for 5–6 km altitudes).

Summing up Eqn (2.4.1) over ω from 0 to $\omega_0 = 10^7$ s^{-1} and also taking into account that $\sin\alpha = \cos\theta$ and the total number of ionization electrons in the shower is W_0/I, where $I = 30$ eV, we obtain the modulus of the resulting amplitude (V m^{-1}) in the form

$$E = \frac{q\omega_0^2 R_\delta W_0}{8\pi\varepsilon_0 c^2 R_0\, I}\,\cos\theta\,. \qquad (2.4.3)$$

Substituting into Eqn (2.4.3) the characteristic values and physical constants given above, we obtain for a particle of energy $W_0 = 10^{17}$ eV and $R_0 = 3\times10^3$ m the value $E = 0.05$, which coincides with the field strength measured in papers [26, 27].

As the flux of particles with energy $W_0 = 10^{17}$ eV is about 3–4 events per hour inside a solid angle 1 sr for a detector with a characteristic area of 10 km^2, for the emission beam width $2\theta = 20^\circ$ one should expect to see one event every 3 hours. So it is clear that there is a high probability that under thunderstorm cloud conditions a giant radio pulse accompanying the air shower can be registered. For the example considered above (2.4.3), the frequency range for which the total amplitude can be evaluated by arithmetically summing up elementary amplitudes (2.4.1) lies within the limits $0 < \nu < 1.5$ MHz. The phase difference for elementary amplitudes from a broader frequency interval exceeds $\Delta\varphi = \pi$ and hence negatively contributes to the resulting amplitude.

2.5 Radio emission by the current of the shower δ-electrons

Apparently, the mechanism of radio emission from a shower in which the elementary act is the breaking of δ-electrons was first suggested in [32]. However, in this paper, the theoretical total intensity proved to be well overestimated due to the neglect of the radiation field phase, which was discussed in [22] in more detail. The point here is that by considering the radiation act by an individual δ-electron within the framework of classical electrodynamics for wavelengths $\lambda \gg R_\delta$, i.e. much exceeding the free path in the medium, one should make allowance for contributions to the total intensity of opposite signs, corresponding to the beginning of the motion with a positive acceleration and to the subsequent stages with a negative acceleration. The significance of this effect increases with the wavelength. Moreover, account should be taken of the emission from those particles that transmitted a fraction of their energy to a δ-electron, thereby changing the character of their motion.

Estimates obtained for the radiation field, which take into account this effect, indicated [22, 23] that the radio emission intensity connected to the breaking of δ-electrons is negligible. Over the subsequent 30 years, this mechanism was abandoned.

This mechanism was addressed anew in connection with the possibility of detecting very high energy showers [10–12]. In paper [12], the authors evaluated the resulting radiation field as a sum of amplitudes of those components of the decomposition for which the phase difference $\Delta\varphi = 2\pi\lambda/L$ does not exceed π along the entire shower path. Clearly, this necessitates that the wavelength range registered by the detector satisfies the inequality $\lambda > 2L$, where L is the shower path over the length of which the number of particles differs from its maximum value by not more than e times. The radiation in this case is said to be quasi-coherent (see above). In other words, to evaluate the field strength within the frequency interval $0 < \nu < \nu(L)$, it is sufficient to sum up the decomposition amplitudes ignoring the phase. Furthermore, the authors of [9] discovered that the spatial-frequency emission diagram proves to be similar to that of an elementary dipole, with the maximum being perpendicular to the shower axis.

Papers [10, 11] revealed that the radiation process considered above in fact reduces to the motion of a current pulse along the shower axis. The excess negative charge, the radiation from which was discussed in Section 2.1, has no direct connection to this radio emission mechanism. So the calculation of the radiation field comes down to finding the current density and to its substitution into the well-known formulas of classical electrodynamics. The radiation process in this treatment has much in common with the phenomenon of passing a very short pulse of current through a conductor.

To simplify the physical model and make numerical estimates, the shower disk in [10, 11] is taken as a material point, and the current density is expressed through the δ-function. Such a representation is quite acceptable since according to the quasi-coherent condition for the given wavelength range ($\lambda > 2L$), the shower cross section is $d \ll \lambda < L$.

For such an analogy, the electric current density can be represented in the form

$$\mathbf{J} = q\delta(\mathbf{r}_i - \mathbf{r}_{0i})\sum_{i=1}^{N}\mathbf{v}_i\,, \qquad (2.5.1)$$

where N is the number of δ-electrons crossing the conditional plane S_0 perpendicular to the shower axis and located at a distance z_0 from the coordinate frame origin. It is known that in this case at a sufficiently large distance $\mathbf{R} = \mathbf{R}_0 - \mathbf{r}$ from the system of charges, the Fourier component of the vector potential $\mathbf{A}(\omega)$ can be presented in the form (see, e.g., [30])

$$\mathbf{A}(\omega) = \frac{\exp(\mathrm{i}kR_0)}{4\pi\varepsilon_0 c^2 R_0}\int\mathbf{J}(\omega)\,\exp(\mathrm{i}\mathbf{kr})\,\mathrm{d}V\,, \qquad (2.5.2)$$

where $\mathbf{R}_0$ is the radius-vector of the point of observation and $\mathbf{r}_i$ is the radius-vector of the charge in the chosen frame. To find the Fourier component of the current density

$$\mathbf{J}(\omega) = \int\mathbf{J}(t)\exp(\mathrm{i}\omega t)\,\mathrm{d}t \qquad (2.5.3)$$

we determine the vector $\mathbf{J}(t)$, which is the sum of the projections on the axis z of elementary currents produced by separate δ-electrons. Clearly, due to the chaotic distribution of velocities $\mathbf{v}_i$ relative to the axis z, the sum of projections $\mathbf{v}_i$ on the other axes is zero. The number of δ-electrons acquiring kinetic energy in the limits from W to $W + \mathrm{d}W$ in passing by the shower disk with the number of particles $f(z_0)$ an elementary length $\mathrm{d}z$, is

$$\mathrm{d}N(W) = A_1 mc^2 f(z_0)\ \frac{\mathrm{d}W}{W^2}\ \mathrm{d}z\,,$$

where $A_1 = 2\pi Z n r_0^2$, and $\beta = 1$ (see, for example, [34]). Then taking into account Eqn (2.5.1) the current density $\mathrm{d}\mathbf{J}$, produced by the $\mathrm{d}N$ electrons in the conventional cross section S_0 (Fig. 2) located at the distance z from the path length $\mathrm{d}z$, will be expressed as the sum

$$\mathrm{d}J = \delta(\mathbf{r} - \mathbf{r}_0) f(z_0)\, A_1 mc^2\, \mathrm{d}z \int_{W_{\min}(z)}^{W_1} \frac{v(z_0)}{W^2} \cos\varphi\, \mathrm{d}W\,, \tag{2.5.4}$$

where W_1 is the maximum possible energy the shower particle passes to the δ-electron, and $W_{\min}(z)$ is the minimum energy necessary for the δ-electron to propagate the distance $z/\cos\varphi$ between the element $\mathrm{d}z$ and the imaginary cross section S_0. Its value can be determined from the relation $z = R_\delta(\gamma)\cos\varphi$ (see below). The flight angle φ of the δ-electron relative to the direction z in the energy range under study can be expressed by the formula $\cos^2\varphi = (\gamma - 1)/\gamma$, where $\gamma = (1 - \beta^2)^{-1/2}$.

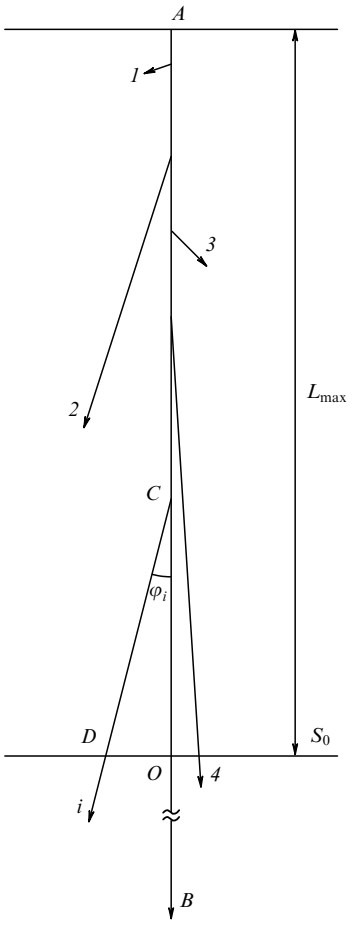

Figure 2. On the δ-electron current density calculation: S_0 — the conventional plane; AB — the shower particle trajectory; O — the intersection point of the plane S_0 by the shower particle; *1–4*, i — trajectories of some δ-electrons; C — the location of the atom from which one of the δ-electrons was knocked out (the electron energy at this point is W), D — the electron crossing point of the plane S_0. $L_{\max} = z_{\max}$ is assumed.

The free path $R_\delta(\gamma)$, depending on the medium density and original energy of the δ-electron, is described by the well-known formula for the ionization losses, which can be presented here in the convenient form

$$R_\delta = -\frac{1}{A}\int_{\gamma_1}^{\gamma_0} \frac{(\gamma^2 - 1)\,\mathrm{d}\gamma}{\gamma^2 \ln\left[m^2c^4(\gamma - 1)^2(\gamma + 1)/I^2(z_1)\right]}\,, \tag{2.5.5}$$

where γ_1, γ_0 is the total δ-electron energy at the beginning and the end of the path, respectively, expressed in units of γ. To find the value $W_{\min}(z)$ or, correspondingly, $\gamma_{\min}(z)$ from the condition $z = R_\delta(\gamma)\cos\varphi$, it is necessary to put the value of γ_0 equal to unity in Eqn (2.5.5). The δ-electron velocity $v(z_0)$ at the moment it crosses the plane S_0 will depend on the initial energy γ_1 and distance between the element $\mathrm{d}z$ and the crossing point of the plane, i.e. $v(z_0) = v(\gamma_1, z) = c(\gamma_0^2 - 1)/\gamma_0$, where c is the speed of light. Then according to Eqn (2.5.4) we obtain

$$J = A_1 f(z_0)\, q\delta(\mathbf{r} - \mathbf{r}_0) \int_{z_{\max}}^{z=0} \mathrm{d}z \int_{\gamma_{\min}(z)}^{\gamma_1} \frac{v(\gamma_1 z)\,\mathrm{d}\gamma}{(\gamma - 1)^{3/2}\gamma^{1/2}}\,. \tag{2.5.6}$$

The value of $z_{\max} = R_\delta(\gamma_1)\cos\varphi(\gamma_1)$ can also be derived from Eqn (2.5.5).

The Fourier component of the current density in accordance with Eqn (2.5.3) is

$$\begin{aligned} J(\omega) &= A_1 qF(\gamma_1) \int_{-\infty}^{\infty} \delta(z - ct) f(ct)\, \delta(x)\, \delta(y) \exp(\mathrm{i}\omega t)\, \mathrm{d}t \\ &= \frac{A_1}{c}\, qF(\gamma_1) f(z_0)\, \delta(x)\, \delta(y) \exp\frac{\mathrm{i}\omega z}{c}\,, \end{aligned} \tag{2.5.7}$$

where $F(\gamma_1)$ is the value of the double integral in Eqn (2.5.6).

Substituting Eqn (2.5.7) into (2.5.2), we obtain the vector potential

$$\begin{aligned} A(\omega) = \frac{A_1 qF(\gamma_1)}{4\pi\varepsilon_0 c^3 R_0} \exp(\mathrm{i}kR_0) \int_{-\infty}^{\infty} f(z) \\ \times \exp\left[\mathrm{i}kz(1 - \cos\theta)\right] \mathrm{d}z\,, \end{aligned} \tag{2.5.8}$$

where θ is the angle between the shower axis and the direction to the observer, $k = \omega/c$. The field strength amplitude can be found using the expression

$$\left|\mathbf{E}(\omega)\right| = \left|\mathbf{A}(\omega)\right| \omega \sin\theta\,.$$

To evaluate $E(\omega)$, we choose the cascade function in the form $f(z) = 0.5N_0(1 - \cos Bz)$, which, within the interval $-z_0 \leqslant z \leqslant z_0$, for our purposes quite satisfactorily reproduces the main properties of the cascade function for the primary particle with energy $W_0 = 10^{20}$ eV, assuming $Bz_0 = \pi$ and $z_0 = 6 \times 10^3$ m. Let us suppose that all stages of the air shower occur in the atmosphere (i.e. it does not strike the soil), and let us also take into account $F(\gamma_1) \approx c/A_1$. Then from Eqn (2.5.8) we derive

$$\left|E(\omega)\right| = \frac{q\omega N_0 B^2 \sin k_1 z_0}{4\pi\varepsilon_0 c^2 R_0 k_1 (B^2 - k_1^2)}\,, \tag{2.5.9}$$

where $k_1 = k(1 - \cos\theta)$. Eqn (2.5.9) implies that at small θ (i.e. if $k_1 \ll B$), the strength is $E(\omega) \sim \omega$. At high frequencies ($k_1 \gg B$) the field strength is $E(\omega) \sim \omega^{-2} \sin k_1 z_0$ i.e. the radiation intensity rapidly falls off as the frequency increases. If $k_1 = B$ the field strength attains a maximum, and after eliminating the ambiguity in Eqn (2.5.9) is expressed in the form $|E(\omega)| = q\omega N_0 z_0 \sin\theta / 8\pi\varepsilon_0 c^2 R_0$ for frequencies close to $\omega_1 = 1.5 \times 10^{-5}$ s^{-1}. After substituting the characteristic values $W_0 = 10^{20}$ eV, $q = 1.6 \times 10^{-19}$ C, $N_0 = 10^{11}$, $z_0 = 6 \times 10^3$ m, $\sin\theta = 1$, $1/4\pi\varepsilon_0 = 9 \times 10^9$ m F^{-1}, $c = 3 \times 10^8$ m s^{-1}, we find that $E(\omega_1) \approx 70$ μV m^{-1} MHz^{-1}, i.e. approximately the same result (for the energy chosen here) as in paper [12], where a simpler but physically more visual model is employed.

As we already noted above, the important feature for applications is that the spatial radiation distribution (2.5.9) at low frequencies is determined by the factor $\sin\theta$, i.e. has the same form as the elementary dipole [12].

As an example, for a shower with energy $W_0 = 10^{20}$ eV, the paper gives the electromagnetic field strength at a distance of $R_0 = 10$ km from the axis. It is 100 μV m^{-1} MHz^{-1}. As the emission maximum lies at wavelengths of 10–12 km, one should bear in mind that $R_0 = 10$ km lies outside the wave zone and such a distance is chosen for convenient comparison with other results.

2.6 Radio emission due to cyclotron coherent radiation

A charged particle moving in a magnetic field deviates from rectilinear motion and thus radiates electromagnetic waves. This emission is called cyclotron (for non-relativistic particles) or synchrotron radiation (for relativistic particles). If the particle velocity is close to the speed of light, the emission diagram has an angular width of order $1/\gamma$. For example, for a particle of an air shower with a characteristic energy in the maximum of ~ 70–80 MeV ($\gamma \sim 150$), the angular size of the emission cone is $\sim 0.2^\circ$. The intensity I of particle radiation is proportional to the particle's charge, i.e. $I \sim (Ne)^2$, and for a broad air shower could be very high. However, there are several factors impeding the coherent summation of the individual particle fields. First, the shower charged particles are intensively scattered in collisions with neutral atoms of the medium. Second, the air shower has a finite thickness and a large cross section. All these significantly destroy the conditions for coherent radiation in the meter wavelength range and lead to a decrease in the electromagnetic radiation intensity.

According to calculations [35], the angle of synchrotron radiation from a broad air shower taking into account the above factors lies within several degrees. So radio emission due to this mechanism can not be used for high-energy cosmic ray detection. Yet there is, however, another point of view on the possibility of using this mechanism [36].

If the observer is in the plane perpendicular to the shower axis and far away from it, at low frequencies (~ 50–10 kHz) the phase difference of the electromagnetic fields for any particle will not exceed π, when the emitting particle is within the shower region L satisfying the condition $\lambda > 2L$ (see Section 2.5).

The wave zone for this mechanism [36], as in the previous case (Section 2.5), lies at $R_0 > 100$ km. For such a remote observer, the angle between the vertical shower axis and the direction to the observer is close to $\pi/2$. All charged particles of the shower (i.e. electrons and positrons) contribute to the total intensity. In the Earth's magnetic field these particles move in the direction determined by the sign of their charge. So the direction of the radiation field strength vector for all particles at the point of observation will be the same.

Avalanche electrons of mean energy $W_1 \sim 50$ MeV ($\gamma \approx 100$) move along an arc of radius $a = mv\gamma/eB \approx 1700$ m and length $S \approx W_1/(\partial W/\partial x) \approx 200$ m (according to the well-known expression for ionization losses $\partial W/\partial x \approx 2$ MeV g^{-1} cm^{-2}). To simplify estimates we shall assume a vertical shower motion. In this case we need only the electromagnetic energy radiated perpendicular to the shower axis. The radiation field produced by a point-like source moving along an arc of arbitrary length is well known [37]. However, in this case the results can be represented in a form more convenient for analysis. This is possible since we are interested only in the low-frequency part of the spectrum. The calculation of the field in the far zone is simplified because $S \ll a \ll R_0$ and the value of the scalar product $(\mathbf{n}, \mathbf{a})$ entering the expression for the field strength does not virtually change during the integration.

For this we represent the electron (positron) velocity in the form of a symmetric step function $U(t)$:

$$\mathbf{v} = \mathbf{v}_1(t) + \mathbf{v}_2(t) = \mathbf{p}v\big[1 - U(t)\big] + \mathbf{q}vU(t)\,,$$

where v is the absolute value of the particle velocity, and $\mathbf{p}$ and $\mathbf{q}$ are the unit vectors for the region of motion $t < 0$ and $t > 0$, respectively. Within the framework of this model we shall assume that inside the region $-\infty < t < \infty$ (except for $t = 0$) the electron moves uniformly and straight by, i.e. $|\mathbf{v}_1| = |\mathbf{v}_2| = v$, and at the moment $t = 0$ the electron is in the middle of the infinitesimal arc S (Fig. 3). Then the acceleration is $\dot{\mathbf{v}} = v(\mathbf{q} - \mathbf{p})\,\delta(t)$, where $\delta(t)$ is the delta-function. Such an idealized representation of the motion characteristics is quite admissible within the estimates accuracy since under the coherence condition the time of motion S/c is much shorter than the period of the oscillatory contour of the radio receiver, i.e. $S/c \ll 2L/c \leqslant T$.

In this case the Fourier component of the field strength is

$$\mathbf{E}(\omega, \mathbf{n}) \approx \frac{e\exp(\mathrm{i}kR_0)}{4\pi\varepsilon_0 cR_0} \int_{-\infty}^{\infty} \frac{\big[\mathbf{n} \times \big[(\mathbf{n} - \boldsymbol{\beta}) \times \dot{\boldsymbol{\beta}}\big]\big]}{(1 - \boldsymbol{\beta}\mathbf{n})^2} \times \exp\left[\mathrm{i}\omega\left(\tau - \frac{\mathbf{na}}{c}\right)\right] \mathrm{d}\tau\,, \qquad (2.6.1)$$

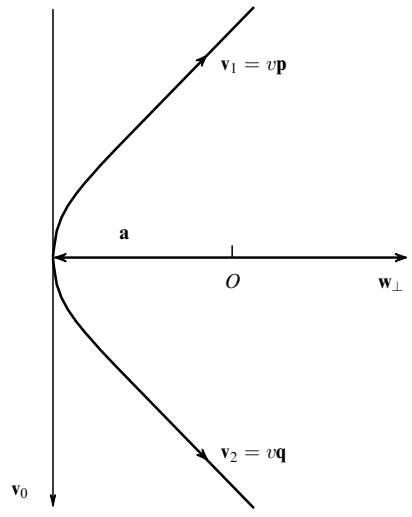

Figure 3. Motion of a charged particle in the Earth's magnetic field. The unit vectors $\mathbf{p}$ and $\mathbf{q}$ correspond to the trajectory directions at the beginning and the end of the path, respectively.

where all quantities are taken at the moment $\tau = t - R/c$. Besides, $\dot{\boldsymbol{\beta}} = \beta\delta(t)\,(\mathbf{q} - \mathbf{p})$, $\boldsymbol{\beta} = \mathbf{v}/c$, $\mathbf{n} = \mathbf{R}_0/R_0$, $\mathbf{a}$ is the radius-vector of the particles, and the coordinate frame has its origin in the center of the circle the arc S belongs to. The result of the calculations (2.6.1) can be represented within an insignificant common phase multiplier by the expression

$$\mathbf{E}(\omega, \mathbf{n}) = \frac{e\beta}{4\pi\varepsilon_0 c R_0}\,\frac{(\mathbf{n} - \beta\mathbf{v}_0)\,\mathbf{n}\mathbf{w}_\perp - \mathbf{w}_\perp[1 - \beta\,\mathbf{v}_0\mathbf{n}]}{[1 - \beta\mathbf{v}_0\mathbf{n}]^2}\,, \tag{2.6.2}$$

where $\boldsymbol{\beta}(0) = \boldsymbol{\beta} = \beta\mathbf{v}_0$, according to the definition of the function $U(t)$; $\mathbf{v}_0$ is the unit vector along the vertical (see Fig. 3); $\mathbf{w}_\perp = \beta(\mathbf{q} - \mathbf{p})$ is perpendicular to $\mathbf{v}_0$ and lies in the plane of the arc, with $|\mathbf{w}_\perp| = \beta S/a$. For the observational direction $\mathbf{n} \| \mathbf{w}_\perp$ and $\mathbf{n} \perp \mathbf{v}_0$ we have

$$\mathbf{E}_\| = -\mathbf{v}_0\,\frac{e\,|\mathbf{w}_\perp|\,\beta}{4\pi\varepsilon_0 c R_0}\,. \tag{2.6.3}$$

The above equation indicates that for a positron the vector $\mathbf{E}_\|$ takes the opposite sign. So the total contribution due to all shower particles in this direction will be close to zero. For the observational direction $\mathbf{n} \perp \mathbf{w}_\perp$ and $\mathbf{n} \perp \mathbf{v}_0$ we have

$$\mathbf{E}_\perp = -\mathbf{w}_\perp\,\frac{e\beta}{4\pi\varepsilon_0 c R_0}\,, \tag{2.6.4}$$

which implies that this field component will not change direction for $e^- \to e^+$, as the direction of the vector $\mathbf{w}_\perp$ would simultaneously turn in the opposite direction. In other words, for the direction normal to the arc plane the radiation intensity will be maximal.

If N_0 is the total number of particles in the shower, then $N_0 L/S$ particles contribute to the field amplitude (2.6.4) along the path L. Finally we arrive at

$$\mathbf{E}_\perp^{\max} = \frac{N_0 L e^2 \mu_0 H}{4\pi\varepsilon_0 c^2 R_0 m\gamma}\,. \tag{2.6.5}$$

Substituting into (2.6.5) the characteristic values $L = 6 \times 10^3$ m, $N_0 = 10^{12}$ (for a particle with energy $W_0 = 10^{21}$ eV), $e = 1.6 \times 10^{-19}$ C, $\mu_0 = 4\pi \times 10^{-7}$ Hn m^{-1}, $H = 40$ A m^{-1}, $1/4\pi\varepsilon_0 = 0.9 \times 10^{10}$ m F^{-1}, $c = 3 \times 10^8$ m s^{-1}, $R_0 = 10^5$ m, $m = 0.9 \times 10^{-30}$ kg, and $\gamma = 50$ we obtain $|\mathbf{E}_\perp| = 100$ μV m^{-1} MHz^{-1}. This is a high field strength (compared to some other mechanisms) for the 100 km distance. However, it is difficult to accomplish such a radio emission observation. The intensity of atmospheric noise is known to increase as the frequency decreases, and for the above region the pulse amplitude can be comparable to the signal under study.

2.7 Transition radiation by excess shower electrons

The possibility of using transition radiation due to excess electrons of the shower for cosmic ray detection was first mentioned in [6]. However, this hypothesis has rarely been invoked in subsequent years [38 – 40]. This radio emission mechanism was considered responsible for the spectral intensity growth at low frequencies. As this frequency range was believed to be hardly promising for the purpose of cosmic ray radio detection, the number of studies of this mechanism was insignificant. These were mostly theoretical papers.

For example, in [38] a theoretical analysis was carried out of the Cherenkov [6], geomagnetic [7], and transition radiation mechanisms for frequencies 10 kHz, 1 MHz and beyond. In particular, one of the results is the conclusion that the dipole current mechanism dominates at high frequencies ($\sim$ 100 MHz). The author of [38] argues that as the collision time τ of the shower disk with the Earth lies within $0.1 < \tau < 1$ μs, the spectral intensity maximum must occur in the frequency range 1 – 10 MHz. Furthermore, an analysis showed that at large distances from the shower (1 – 10 km), transition radiation dominates in the frequency range $\sim$ 1 MHz.

Paper [39] reported the experimental study of the radio emission at 50 kHz frequency. The experimental setup involved a vertical antenna with a band filter. The author argues that the amplitude is well consistent with the theoretically predicted model for transition radiation. However, an analysis of this paper shows that the experimental method employed to study the radiation field at low frequency does not correspond to the purpose pursued. For example, the results [39] should be connected to the Coulomb field zone, and it hardly makes sense to compare them with theoretical results for the far zone (see [41] for more detail).

In a recent paper [42], spatial-frequency diagrams of the shower transition radiation were obtained taking into account the soil conductivity. The radiation is revealed to possibly have a strong beaming. We shall not reproduce here the rather cumbersome calculations and formulas obtained in this paper but will restrict ourselves to briefly considering the result. The continuation of the shower axis projection on the Earth's surface is coincident with the radiation maximum direction. Figures 4a – f demonstrate some spatial-frequency emission diagrams for different θ and frequencies ω_0.

The ratio of intensities corresponding to the maximum and minimum of the spatial diagram can be much larger than 10. To find such diagrams depending on the frequency and the shower axis inclination angle, in [42] the Earth's surface is substituted by an ideal conductor, which is well known to be quite justified for low and medium frequencies. In this case the radiation field of the charged particle crossing the Earth's surface is equivalent to the bremsstrahlung field in an 'immediate' stopping of this particle and its electric image on the separation boundary [8]. Thus the transition radiation model comprises three stages of the excess electron motion:

1) momentary acceleration up to a velocity of about $c = 3 \times 10^8$ m s^{-1}. This stage corresponds to excess electron creation (as well as positron disappearance);

2) nearly uniform motion over a straight interval;

3) momentary stopping on the separation boundary.

The electric image of the electron passes through similar stages. The radiation field in this model is the result of the superposition of the fields of all the shower's excess electrons. The summation in [42] takes into account both the directional character of the field and its phase. This agrees with the conclusion on the spectral intensity maximum location at $\sim$ 0.75 MHz. Clearly, the same result follows from considering the radiation quasi-coherence condition for an observer in the Earth's plane. For example, in the vertical motion of an ideally thin shower disk, the wavelength range of the quasi-coherent radiation is determined by the condition $2d < \lambda < \infty$, where d is the shower disk diameter. In this case, the phase difference of the fields produced by charges located at opposite disk points is less than π. So if $d \approx 200$ m,

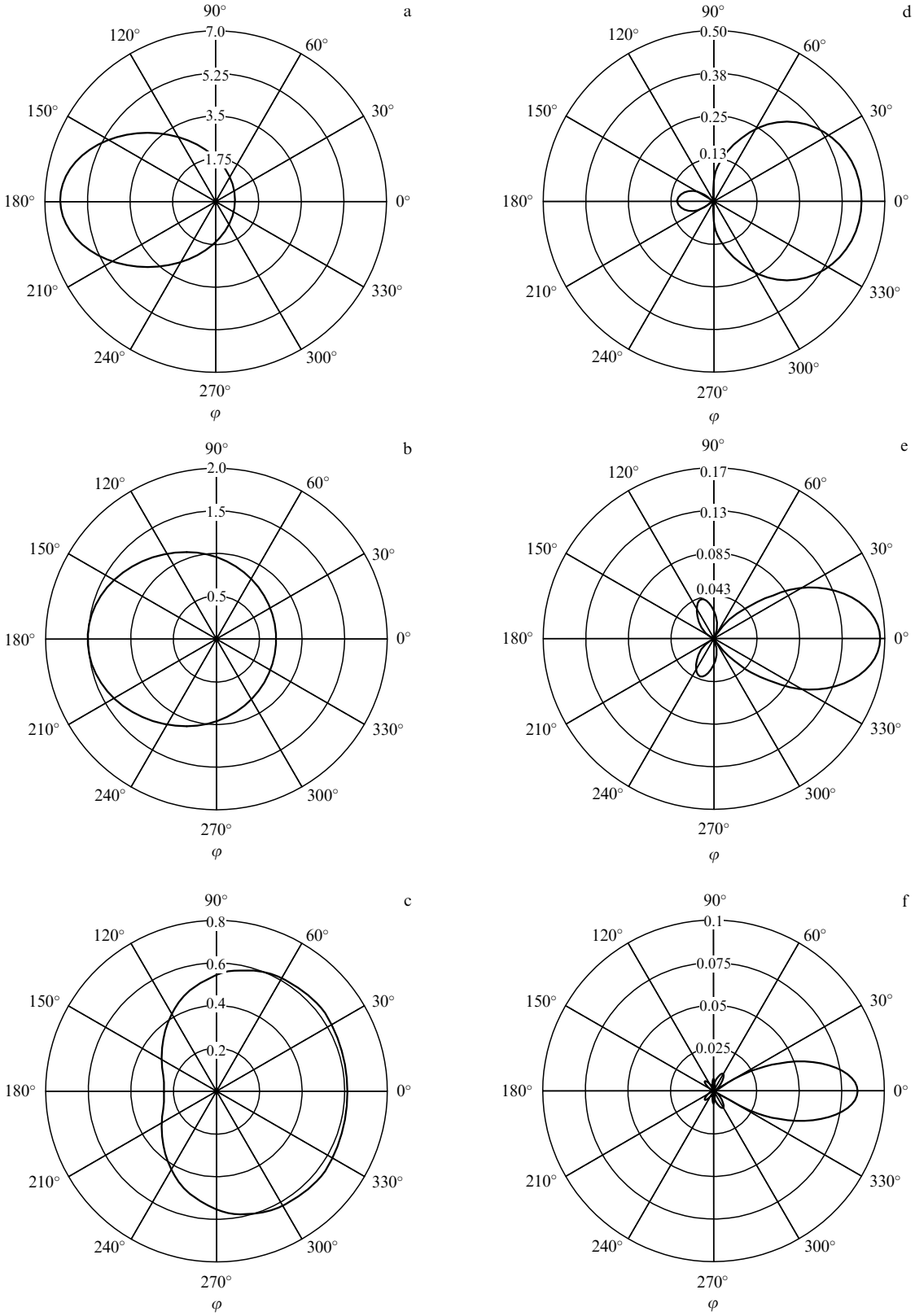

Figure 4. Characteristic emission directivity diagrams for different frequencies and angles θ (see the text): (a) $\theta = \pi/6$, $\omega_0 = \pi\sqrt{3}/12$; (b) $\theta = \pi/6$, $\omega_0 = 3\pi\sqrt{3}/12$; (c) $\theta = \pi/6$, $\omega_0 = 4\pi\sqrt{3}/12$; (d) $\theta = \pi/6$, $\omega_0 = 6\pi\sqrt{3}/12$; (e) $\theta = \pi/6$, $\omega_0 = 9\pi\sqrt{3}/12$; (f) $\theta = \pi/4$, $\omega_0 = 9\pi(\sqrt{2}+1)/12$.

then $\lambda > 400$ m, which corresponds to the medium wavelength range (~ 0.7 MHz).

The absolute values of the field spectral component obtained in [42] are relatively small. For example, for a primary energy $W_0 = 10^{20}$ eV and a distance to the point of observations $R_0 = 10$ km, the field strength is ~ 10 μV m^{-1} MHz^1. This is an order of magnitude smaller than for the cyclotron radio emission.

2.8 Transition radiation of the air shower quasi-static dipole

The radio emission intensity produced by this mechanism is about an order of magnitude higher than the transition radiation from excess electrons (see Section 2.7). To estimate the field spectral component inside the wave zone, the air shower can be modeled as follows [9]:

1. The air shower is an infinitesimally thin disk with the rms radius $r_0 = 100$ m. Positrons and electrons are uniformly distributed over its surface such that it is neutral as a whole.

2. The shower particle number as a function of the altitude z is described by the cascade function $f(z)$, which in this model is determined with sufficient accuracy by the dependence $f(z) = N_0 \exp(-\alpha^2 z^2)$, where $\alpha = 0.33 \times 10^{-3}$ m^{-1} is found from the condition that the active part of the path (where the number of particles changes by e times) is ~ 6 km. The distance z the shower covers is counted from the point at which the particle number reaches a maximum.

3. The vertically moving neutral disk is split by the horizontal component of the Earth's magnetic field across its motion into two disks of opposite signs. The electric moment of the dipole thus formed is $0.5N_0 q f(z)\, d$, where d is the distance established between the centers of the oppositely charged disks and $0.5N_0 q f(z)$ is the total disk charge.

4. The shower disk moves uniformly with a velocity of $v \approx 3 \times 10^8$ m s^{-1} along a trajectory of a variable curvature radius. Such a motion is due to a slight deviation in the Earth's magnetic field and ionization losses. About half the shower electrons have the initial energy $\gamma \approx 200$ ($\sim 10^8$ eV). For ultra-relativistic particles, ionization losses are independent of the velocity and are equal to ~ 0.25 MeV m^{-1} under normal conditions.

5. The current density produced by the charged disk of one sign is expressed through the δ-function

$$\mathbf{j} = \frac{1}{2}\,\mathbf{c} f(z)\, q\delta\big(\mathbf{r}' - \mathbf{r}(t)\big)\,,$$

where $\mathbf{r}'$ is the radius-vector of an arbitrary point in space, $\mathbf{r}(t)$ is the equation of motion for the shower disk, and $q = 1.6 \times 10^{-19}$ C. Such an approximation is quite possible since for the radiation field inside the far zone, $|\mathbf{r}| \ll \lambda \ll R_0$, where R_0 is the distance to the observer.

Consider the principal stages of radio emission intensity calculation for a vertical shower. According to the accepted model, during the time of motion the electrons (positrons) spend their energy $W_1 = 10^8$ eV for ionization and travel a distance of 400 m. In an arbitrary segment of the path $\mathrm{d}z$ they shift across its motion and across the horizontal component of the Earth's magnetic field by $\mathrm{d}y = \mathrm{d}z \sin\psi$, where $\psi = \psi(z)$ is the angle the instantaneous curvature radius of the trajectory $R(z) = mc\gamma(z)/qB$ makes with the horizon. So the total displacement $d/2$ reads

$$\frac{d}{2} = \int_0^{396} \sin\left(\int_0^z \frac{\mathrm{d}z'}{R(z')}\right)\mathrm{d}z\,, \qquad (2.8.1)$$

where the integration limit $z = 396$ m is chosen from the condition that, before striking the Earth, the shower disk velocity is still close to the speed of light ($\gamma \geqslant 2$).

Substituting the necessary values into Eqn (2.8.1) yields $d = 50$ m. This means that two oppositely charged disks separated by $d = 50$ m will encounter the Earth's surface. The fact that the disks overlap, leading to the intensity decrease, is accounted for by introducing the phase $\exp[\mathrm{i}k(R_0 \pm d\cos\varphi)]$, where φ is the angle between the line of sight $\mathbf{n}$ and the dipole axis. Expressing the current density through the δ-function and assuming high soil conductivity (which is justified at frequency ~ 1 MHz), then according to [30, 8] we have

$$E(\omega) = \frac{2\mathrm{i}\omega q N_0 \exp(\mathrm{i}kR_0)}{4\pi\varepsilon_0 c^2 R_0}\int \exp\left(\frac{\mathrm{i}\omega z}{c}\right) f(z) \times \left[\exp(\mathrm{i}kd\cos\varphi) - \exp(-\mathrm{i}kd\cos\varphi)\right]\mathrm{d}z\,, \qquad (2.8.2)$$

where the product $\mathbf{kz} = 0$ and $\big|[\mathbf{n} \times \mathrm{d}\mathbf{z}]\big| = \mathrm{d}z$ since the shower axis is almost vertical, and the observer is inside the wave zone on the Earth's surface, so the condition $\mathbf{k} \perp \mathbf{z}$ always holds. In addition, the integral over variables x and y (which are the arguments of the δ-function only) is equal to unity.

If the shower dissipates before reaching the Earth, the integration limits lie within the interval $-\infty < z < \infty$. In that case Eqn (2.8.2) entails

$$E(\omega) = \frac{\omega q N_0}{\sqrt{\pi}\varepsilon_0 c^2 R_0\,\alpha}\exp\left(-\frac{\omega^2}{4\alpha^2 c^2}\right)\sin(kd\cos\varphi)\,. \qquad (2.8.3)$$

The maximum of Eqn (2.8.3) is attained at the frequency $\omega = \sqrt{2}\alpha c \times 1.4 \times 10^5$ s^{-1}. Substituting into (2.8.3) the characteristic values $N_0 = 10^{12}$ — the electron number at the maximum [34] for the primary particle energy $W_0 = 10^{21}$ eV, $R_0 = 10^4$ m — the distance to the observer, $d = 50$ m, $\varphi = 0$, $\alpha = 1/3 \times 10^{-3}$ m^{-1}, $c = 3 \times 10^8$ m s^{-1}, $k = \omega/c$, $\omega = 1.4 \times 10^5$ s^{-1}, $q = 1.6 \times 10^{-19}$ C, $(4\pi\varepsilon_0)^{-1} = 0.9 \times 10^{10}$ m F^{-1}, we obtain

$$\big|E(\omega)\big| = 65\ \mu\mathrm{V\ m^{-1}\ MHz^{-1}}\,.$$

The integration limits in Eqn (2.8.3) should be taken inside the interval $-\infty < z = 0$ since for particles with $W_0 \sim 10^{20} - 10^{21}$ eV the shower maximum occurs immediately close to the Earth's surface. In this case to calculate (2.8.3) it is convenient to utilize the interval expansion in even powers $1/x$ [123] where $x = \mathrm{i}\omega/\alpha c\sqrt{2}$. Then

$$E(\omega) = \frac{2\mathrm{i}\omega q N_0\sqrt{\pi}}{8\varepsilon_0 c^2 R_0 \alpha}\exp\left(-\frac{\omega^2}{4\alpha^2 c^2}\right) \times \left[1 - \frac{\exp(-x^2/2)}{x\sqrt{2\pi}}\left(1 - \frac{1}{x^2} + \frac{3}{x^4} - \ldots\right)\right]\sin(kd\cos\varphi)\,. \qquad (2.8.4)$$

In determining the main term in Eqn (2.8.4) we should take into account that by expressing the current (of positrons and electrons) through the δ-function, we constrain the wavelength range considered in this model. As the disk size is $2r_0 = 200$ m, the amplitudes of harmonics (2.8.2) for $\lambda \geqslant 400$ m can be added ignoring the phase. This inequality corresponds to the frequency range $0 < \omega_0 < 4 \times 10^6$ s^{-1}. For this frequency the value of $1/x^2$ is of the order of 10^{-3}, so in the parenthesis of expansion (2.8.4) we may retain only the zero term:

$$\big|E(\omega)\big| = \frac{N_0 q}{2\pi\varepsilon_0 c R_0}\sin(kd\cos\varphi)\,. \qquad (2.8.5)$$

An ordinary antenna like the half-wave dipole frequently used in publications cited above has a working frequency

band $\Delta\omega/\omega \approx 0.1$. Hence the more precise definition of the lower and upper limits for the validity of Eqn (2.8.5) is meaningless. The argument of the sine function in Eqn (2.8.5) is 0.66 even for $\cos\varphi = 1$. So at frequencies $0 < \omega < \omega_0$ the spatial emission diagram has a shape typical of an elementary dipole. After substituting the physical quantities already used in calculating (2.8.2), we find the maximum value (at $\varphi = 0$) of the field spectral component $E(\omega) \approx 700$ μV m^{-1} MHz^{-1} for $R_0 = 10^4$ m and $W_0 = 10^{21}$ eV. This value is about an order of magnitude higher than (2.8.3).

An analysis of the obtained results implies that paper [9] may stimulate the relevant experimental studies. The point is that according to data on the frequency distribution of atmospheric noise [43, 44], their intensity minimum occurs at frequencies of about 1 MHz and is coincident with the position of the radiation intensity maximum for this radio emission mechanism. Moreover, the atmospheric noise decreases by about 30 dB in the polar latitudes. At the most favorable time of day and season, the strength of the atmospheric fields for the moderate zone of the European part of Russia is ~ 1 μV m^{-1} MHz^{-1} [43, 44]. Evidently, this is much lower than the signal field strength from the example given above even at distances of 100 km from the shower.

Such a situation is very favorable for experimental studies. Consider the following example. Let four radio receivers with simple antennas and an autonomic power supply be located at the corners of a square with sides of 70 km. All these can be brought outside the region of technical noise, for example in the polar latitudes of the Pacific ocean. An air shower within a circle 70 km in radius with a center coincident with the square's center, in the worst case would be within 40 km of one of the antennas. If the particle energy is $W_0 = 10^{20}$ eV, then, as we found above, the radiation field strength is 15 μV m^{-1} MHz^{-1}. This value exceeds the atmospheric noise field strength for polar zones by one to two orders. It is well known (see [45] for example) that on average one particle with energy $W_0 = 10^{20}$ eV falls per square km of the Earth's surface per hundred years. This means that by utilizing the setup under consideration, one can register at least 150 particles per year. To evaluate the significance of that result correctly, we should add that over the entire history of cosmic ray science only about 15 events with energy $W_0 = 10^{20}$ eV have been registered. The hypothetical setup described here is evidently not yet a detector. Besides the arrival of the particle and the number of particles in the shower maximum, nothing else can apparently be determined. However, it would differ principally from modern detectors by its capabilities at high energies $W_0 > 10^{20}$ eV. An even more significant effect could be achieved by using this hypothetical setup in combination with an ordinary detector, such as ShAL-1000. This should stimulate exploration of the nature of such radio emission.

However, there is a circumstance that must radically change the research method. The point is that no master signal is present in such an experiment, i.e. such a synchronization pulse that is always employed in classical works. In early studies, in view of the small detector area, it was quite easy to place several ionization or scintillation counters or even use for this purpose a traditional detector of charged particles, which not only generated the synchropulse, but also determined the shower energy. The presence of synchropulses in the described experimental scheme would significantly simplify the signal detection. However, its absence can be compensated by other means. Firstly, in the given conditions only a lightning discharge could be the source of a false signal. For example, if in this experiment one takes the antenna in the form of mutually perpendicular frames, then the ratio of currents induced by the radio pulse can be utilized to determine the pulse arrival direction [46]. In other words, the set of antennas plays the role of a direction-finding system. For a remote thunderstorm pulse, all four frames would indicate the same direction. For a local thunderstorm, a powerful pulse is easily distinguished not only by its arrival direction, but by its high amplitude value as well. Secondly, it is well known that a lightning discharge is an intermittent current pulse with a total duration of tens and even hundreds of milliseconds. This is its characteristic feature distinguishing it from an expected signal of simple form and shorter duration.

To conclude, we can briefly mention the possibility of studying air showers in the near zone, i.e. in the region of the Coulomb (quasi-static) field. For example, by measuring the potential near the axis, one can determine the absolute quantity of excess electrons which was estimated in [6]. The excess shower electrons produce a current that can be measured by the induction method. Using the inductance form specially chosen for this purpose, one can find the air shower motion direction [47].

The present review of works on radio emission mechanisms from air showers is not complete. Here we have not considered the papers which, in the author's opinion, are not directly related to studies of the nature of radio emission (such as, for example, [48–50]). However, even this list gives evidence of the diversity of electric processes accompanying air showers.

3. Experimental studies of radio emission from air showers at high frequencies (> 30 MHz)

The stimulating effect of publications [6, 7] has turned out to be quite large. Preliminary results of experimental studies were already published some years later [51]. This was a pattern experiment, and the design of its setup with insignificant modifications was repeated later on in almost every work. This is why the method of the experiment and its results must be described in more detail. The list of the main units of such setups includes:

(1) an antenna (one or more) to register radio pulses;

(2) a scintillation or ionization detector to determine the shower energy and to obtain the synchronizing pulse (master-signal);

(3) an amplifier of radio pulses (radio receiver);

(4) a recording device (for example, an oscillograph);

(5) a scheme for synchronization of the moment the recorder starts up with the moment the slower is registered by the particle ionization detector.

Experimental setup [51] was designed to study showers with energy $10^{15}-10^{16}$ eV. To obtain the master-signal (Fig. 5), the Geiger–Muller counters *2–4* were attached to the coincidence scheme *5*, which turned-on the recording oscillograph *7* only if all three counters *2–4* were triggered. Practically simultaneously, a current pulse was induced in the antenna *A*. After preliminary amplification in unit *10*, it passes through the delay line *9* to the radio receiver *8*. The recording oscillograph *7* was activated by the trigger.

The antenna of the setup comprised 72 half-wave vibrators with the eigenfrequency 44 MHz and the bandwidth $\Delta\nu = 4$ MHz. To form the vertical beam, the antenna

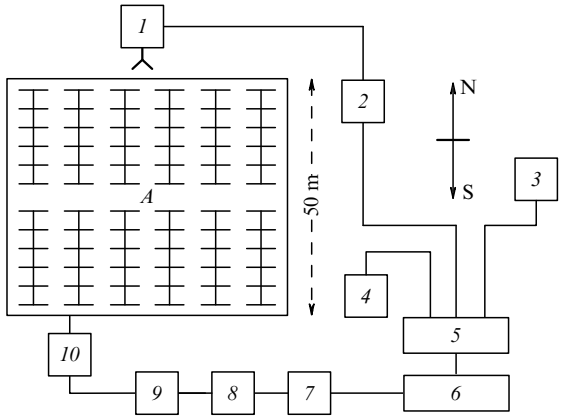

Figure 5. Block-scheme of the experimental set-up for studies of broad air showers with energy $10^{15}-10^{16}$ eV [51]: *A* — multielement antenna; *1* — artificial trigger generator; *2–4* — ionization counters; *5* — coincidence scheme; *6* — turn-on trigger; *7* — oscillograph; *8* — delay line; *9* — radio pulse amplifier; *10* — preamplifier with autonomous power supply.

array was set at $\lambda/8$ above the ground. The aim of the experiment was to check theoretical estimates of the Cherenkov radiation by excess electrons [6, 19]. The identification of this mechanism could be carried out by the character of the radiation field polarization. The field strength vector at the point of observation is known to lie in the plane formed by the particle motion and the line of sight. In addition, it is perpendicular to the wave vector. So if an air shower struck the center of the triangle formed by the counters *2–4*, the dipole orientation shown in the figure would correspond to the signal amplitude maximum. The amplification of such an antenna is estimated to be 21 – 22 dB, which corresponds to a voltage amplification of about 12 times.

In the experiment, 1799 showers were detected, five of which exceeded the rms noise level by 8, 10, 10, 11, and more than 45 times, and corresponded to energies 4×10^{-12}, 5×10^{-12}, 3×10^{-12}, 3×10^{-12}, and more than 20×10^{-12} erg, respectively. All of them arrived within the expected time interval τ 5,4 – 5 μs on the oscillograph scan. In other parts of the 20-μs scan no pulses were registered. Of 1117 artificial triggerings by generator *1*, none of the radio pulses arrived outside the interval τ (Fig. 6a).

The statistical analysis of the remaining 1794 pulses indicated that in most cases they fell within the time interval τ (Fig. 6b). The total signal amplitude inside the interval τ was

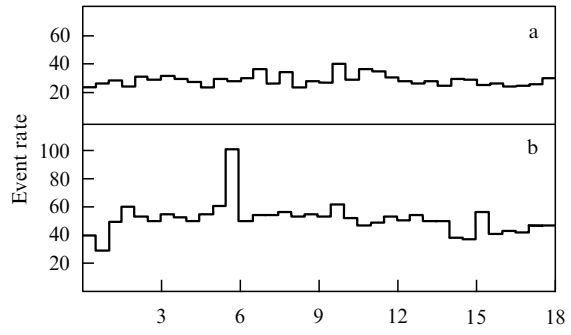

Figure 6. (a) Histogram of 1117 artificially triggered random events. (b) Histogram of 1794 events from a broad air shower. The event rate is plotted along the vertical axis.

four times as much as the rms deviation. On these grounds, the conclusion was made that the pulse series registered was due to radio emission from the air shower.

This experiment was continued and a detailed discussion of its results was published almost two years later [52]. The experimental setup was significantly modified over the two years. Instead of one antenna array, two units were used with mutually perpendicular polarizations (N – S and W – E). Counter *3* was mounted on the opposite side of antenna *A* such that it proved to be at the particle detector's center (see Fig. 5). Moreover, equipment was added allowing studies at a frequency of 150 MHz. The angular size of the major lobes of the directivity diagram for both antennas (44 and 150 MHz) was 10° and 12°, respectively, at the 3 dB level. The noise temperature of the amplifier was less than 450 K. So the noise properties of the entire system were determined by the equivalent temperature of the celestial sphere, which varied within the range $6\times10^3-2\times10^4$ K at a frequency of 44 MHz depending on the sidereal time. The radio receiver sensitivity threshold was determined by the noise and was within the range $(0.8-2.8)\times10^{-12}$ erg. The effective areas of the main (44 MHz) and high-frequency (150 MHz) antennas were 1700 and 170 m^2, respectively. All the systems, including the antennas, were tuned and calibrated using the discrete radio source Cas A.

In the period between November 1964 and March 1965, 4500 events were recorded, 11 of which had an amplitude exceeding the oscillograph scale and arrived within the expected time interval τ 5 – 6 μs. No pulses of such an amplitude were detected in other parts of the sweep from 0 to 5 μs and from 6 to 20 μs. Of 2800 artificial triggerings, no pulses were detected beyond the interval τ as well. The statistical analysis of the events, as in the previous experimental series [51], confirmed with a high probability that they originated from a broad air shower.

Observations at frequencies around 150 MHz were performed to check the condition of coherency. At these frequencies the wavelength ($\lambda = 2$ m) is smaller than the disk size d, and this must substantially violate radiation coherence. Assuming a normal distribution of the excess shower electrons in the longitudinal direction of the disk $N(x) = N_0\exp(-2x^2/d^2)$, at $d = 1$ m for $\lambda = 2$ m a ten-fold signal decrease should be expected. It was revealed that due to a decrease in the effective antenna area, a decrease in the passband width ($\Delta\nu = 1$ MHz), a change of the noise characteristics, etc., the spectral intensity increase in passing from the observation frequency $\nu = 44$ MHz to $\nu = 150$ MHz would generally be insignificant. However, over six weeks no pulses were detected at 150 MHz. At the same time, at 44 MHz the setup registered five high-amplitude events. This allowed the authors to conclude that there was significant coherence violation at high frequencies.

In theoretical paper [7], where the geomagnetic radio emission mechanism was studied, the conclusion was reached that the radiation is polarized in the direction E – W. To test this, both antennas at 44 MHz were carefully calibrated to achieve full identity of the channels. However, the subsequent observation carried out over one week simultaneously in two channels with different polarizations (E – W and N – S) did not reveal a significant difference either in the number of pulses or in their amplitudes.

The amount of energy passing through unit area per unit frequency band over the total time of the process at the

distance r from the observer (erg $\mathrm{cm}^{-2}\mathrm{Hz}^{-1}$) was calculated according to [7] for the 44 MHz range using the expression

$$I_v = 2 \times 10^{-37} N_0^2 J_0^2(0.024a)\left|H_0^1(0.024r)\right|^2 .$$

Assuming the ring radius $a = 17$ m, the distance to the observer $r = 100$ m, the shower number particle $N_0 = 10^6$ and the time of the process of about 10^{-8} s, the spectral intensity will be $I_v = 2 \times 10^{-20}\,\mathrm{W\ m^{-2}\,Hz^{-1}}$ and the total energy released on the antenna's load during the process in the passband 2.8 MHz will be 3.6×10^{-12} erg. This energy being equal to what was observed led the authors to conclude that there is a tight correlation between the realistic radio emission mechanism and the Cherenkov radiation [6, 19] or geomagnetic radiation [7].

A large series of experiments was carried out on the setup of the Skobel'tsyn INP MSU and Kharkov State University (KSU). One of the first papers of KSU [53] aimed to confirm the possibility of registering the radio pulse that accompanies an air shower. The structure of the experimental setup was largely the same as considered in [51]. However, the frequency range 12.7 MHz with a passband width of 2.6 MHz was selected for the studies. Three Geiger – Muller counters and two photo multipliers detecting Cherenkov light flashes from air showers were used to activate the registration system. Based on statistical data on the number of time-coincident events in the optical and radio channel, or in the Geiger – Muller counter and the radio channel, the authors conclude that it is possible to effectively register radio signals in the case where the shower energy is $W_0 > 6 \times 10^{16}$ eV.

This experiment was continued using an upgraded setup to determine the dominant mechanism of the shower radiation [54]. For this, the frequency range, which had been very close to the radio broadcasting frequencies 11.7 – 12.1 MHz in the earlier studies, was shifted to the 20 MHz range with a bandwidth of 1.4 MHz. Two antenna systems used in the setup each included 6 half-wave dipoles. One of them was oriented along the W – E direction, another along the N – S line. The effective solid angle and geometrical area were 0.3 sr and 100 m^2, respectively. The minimum radio emission flux registered by the setup was $1.7 \times 10^{-20}\,\mathrm{W\ m^{-2}\,Hz^{-1}}$. The results of the measurements were evaluated by the count rates in the triple coincidences. The authors argue that the shower radio emission polarized along the E – W direction gives evidence of the dominating role of geomagnetic mechanisms.

Using the complex setup of INP MSU, a series of experimental studies was carried out (mainly in 1967 – 1972) to establish the different characteristics of a radio emission field from a broad air shower [55 – 60]. The particle detector of the complex setup is described in [61] in more detail. The elements of the radio detector [55] included two antennas — wide-band horizontal half-wave vibrators located at distances 60 and 140 m from the setup center. The vibrator eigenfrequency was selected outside the broadcasting radio bands (30.2 MHz). At almost any time of the day, the ionosphere is transparent for these frequencies. The oscillograph DESO-1 was used as a registering device, whose scanning was triggered by a master-signal generated by the particle detector.

Radio emission from the showers was registered over 1100 hours. Only radio pulses arriving during the last 400 hours were fully analyzed. Radio pulses with a signal power 25 times exceeding the noise were analyzed for the whole 1100 hours. In 400 hours of operation, 27 showers with a radio flux of more than 5 times the cosmic radio noise were detected, while over the other 700 hrs, there were 17 broad air showers with a radio flux 25 times the cosmic radio noise flux. As the radio emission predicted in geomagnetic mechanisms [7] is linearly polarized and the field strength is proportional to the sine of the angle between $\mathbf{v}$ and $\mathbf{H}$, in constructing the spatial distribution curves the radio emission power was normalised to the square of the total number of muons or electrons using the relation

$$\psi^2(\theta,\varphi) = \frac{\left|\mathbf{E}(\theta,\varphi)\right|^2}{\left|E_{\max}\right|^2} ,$$

where $\psi(\theta,\varphi)$ is the polarization degree, $\mathbf{E}(\theta,\varphi)$ is the radiation electric field strength, and $E_{\max}$ is the maximum strength of the electric field corresponding to the shower motion in the direction perpendicular to the Earth's magnetic field. The dispersion of the radio emission flux (for one arbitrary chosen distance from the shower) with the normalization N_e^2 is found to be several orders of magnitude higher than the flux dispersion with the normalization N_μ^2. Furthermore, the radio emission normalization ignoring ψ^2 would lead to an additional amplitude dispersion. These facts allow the authors of [55] to conclude that the radio emission flux is linearly polarized and is proportional to N_μ^2. In other words, the number of muons in the shower can be a good measure of the energy W_0 of the primary particle that produced the air shower.

Paper [56] studied the spatial distribution of radio emission in individual air showers. For this the number of vibrators was increased up to nine, with eight of them being oriented in the E – W direction and one in the N – S direction. This was done in order to obtain additional information on the emission polarization.

The measurements show that the spatial emission diagram of air showers is narrow-beamed. For example, at a distance 100 – 500 m from the shower axis, the radiation power decreases by at least an order of magnitude. In addition, the radiation source is at an altitude of a few kilometers. It is also established that at a significant angle between the shower axis and the geomagnetic field ($60^\circ \geqslant (\widehat{\mathbf{vH}}) \geqslant 20^\circ$), the intensity measured does not contradict the geomagnetic hypothesis but does disagree with the Cherenkov radiation from excess electrons. For $18^\circ \leqslant (\widehat{\mathbf{vH}}) \leqslant 30^\circ$ the data for two showers is consistent with the two mechanisms. One shower at an angle between $\mathbf{v}$ and $\mathbf{H}$ of about 10° does not contradict the 'excess' mechanism, but does not correspond to the geomagnetic one.

To determine the polarization of the radiation, it is convenient to use so-called cross-like antennas. Such an antenna consists of two independent perpendicular half-wave dipoles located such that the vibrator centers coincide. Some such antennas were used in [57] to continue studies of the radiation mechanisms. In total, the setup included nine antennas. Only those showers from which pulses were detected by more than three antennas were analyzed. Below we display the distribution of 25 showers according to the number of triggered antennas (Table 2).

For 20 showers, at least one of the constituent vibrators of the cross-like antennas was triggered. The signal amplitudes were compared to theoretical predictions for different radio emission mechanisms. Estimates were made not only for the mechanisms considered in [6, 19] and [7], but also for the geoelectric mechanism [21, 22]. The measurements give evidence for the dominating role of the geomagnetic mechan-

Table 2.

Number of antennas	3	4	5 – 9
Number of showers	6	10	9

ism, although it is most probably not the only one. In particular, at small angles between **v** and **H**, other radio emission mechanisms prevail. Moreover, these measurements confirmed the fact discovered earlier of the sharp drop in radiation intensity at a significant distance from the shower axis. To understand the radio emission mechanism, it is necessary to know the radiation power frequency distribution as well. For this purpose, in addition to the already existing vibrators of eigenfrequency 30 MHz, the complex setup of MSU was completed by a vibrator for the frequency 62 MHz, setting it at a distance of 60 m from the setup center [58]. Eight vibrators (including the short-wave one) were oriented along the geomagnetic parallel, and three along the geomagnetic meridian. The event selection was chosen so that the probability of at least one false alarm was less than 3 %. In the observation period from January to May 1970, 22 showers satisfying the rigorous selection criterion were registered. Analysis of the polarization characteristics and the spatial radio emission distribution at the frequency 30 MHz did not reveal a significant difference between these results and those obtained earlier [57]. For the frequency 62 MHz, the intensity decrease with the distance from the shower is more significant than for 30 MHz. The author argues that this could be connected to the violation of radiation coherency at high frequencies.

From May to September 1971, the complex setup of the INP MSU for air shower studies included a registration system consisting of 11 parallel channels tuned to the frequency 32 MHz and six channels tuned to 58 MHz [60]. Over this period of time ten showers were observed from which radio emission was simultaneously detected at both frequencies, by at least one antenna at 58 MHz and by several antennas at 32 MHz. Only pulses with amplitudes larger than 30 μV at 58 MHz and 50 μV at 32 MHz were analyzed. The total number of particles N_e in these showers varied from 5×10^6 to 6×10^7 and the total number of muons with energy larger than 10^{10} eV fell within the range from 2×10^5 to 10^6. None of the showers considered contradicted the geomagnetic radio emission mechanism. No dependence of the ratio E_{60}/E_{30} on the value N_μ/N_e, the shower age S, and the zenith angle θ was found. By analyzing the relation between the ratio E_{60}/E_{30} and the value of $\sin(\widehat{\mathbf{vH}})$, the authors of [60] came to the conclusion that radio emission mechanisms different from the geomagnetic one in frequency spectrum should exist.

Air shower radio emission spectral distribution studies were continued using the setup of Kharkov State University [62]. The radiation field strength intensity was measured at frequencies 34, 40, 52, 135, and 162 MHz. Over 1155 h of operation, five showers were registered accompanied by radio emission. The common tendency of all the events was a rapid decline of the spectral distribution at frequencies 30 – 50 MHz and its slow variation at high frequencies. These results contradict the data of [63, 64] and to some extent coincide with [60].

A theoretical paper of this group [65] examined the shower radio emission spectral dependence on the distance to the vertical shower axis and on the age characterizing its longitudinal evolution. Calculations of the amplitude-frequency spectrum made allowance for possible coherence of the shower radio emission at meter and decimeter radio wavelengths [6, 19], as well as for the assumption of its form dependence on spatial coherence, i.e. on the phase difference of waves arriving at the observer. In addition, the influence of multiple Coulomb electron scattering on neutral atoms of the medium on the spectral form was taken into account. Only two generation mechanisms, Cherenkov and synchrotron, were considered.

Numerical calculations of spectral functions point to a weak difference between the two coherent mechanisms at the same position of the air shower maximum. A characteristic feature of spatial distribution is a decreasing gap (as the maximum of the shower approaches the Earth) near the axis caused by angular distribution of particles or some irregularities at large distances from the axis which increase in the course of the shower's evolution. In [65], theoretical calculations are compared with experimental results and a qualitative agreement with [62] is pointed out.

The fact should be noted that the above series of works contains very little information on showers with energy in excess of $W_0 = 10^{17}$ eV. This is partially explained by the limits of the ionization detectors of the complex experimental setup. But there is another principally important fact. As the shower energy increases, its maximum approaches the Earth's surface. For example, for a shower with $W_0 = 10^{20}$ eV it lies at a distance of several hundred meters above sea level. From the theoretical point of view [6, 19, 7], the field strength of radio emission from a shower with $W_0 \sim 10^{19}$ eV must exceed by two to three orders the strength obtained in experiments [53 – 62] for $W_0 \approx 10^{16} - 10^{17}$ eV. However, except for rare occasions, such an effect was not observed. This can be clearly explained, however. As we noted above several times, the condition of quasi-coherent radiation holds only for a narrow observation cone. For example, according to estimate [19], the emission angle lies within 1°. If multiple Coulomb scattering is taken into account, in this case the major lobe of the spatial emission directivity diagram will not be too large, as indicated by test results [53 – 62]. So an observer not even very far away from the axis of a shower with $W_0 \sim 10^{18} - 10^{19}$ eV can end up being outside the emission cone when the shower maximum approaches the ground surface.

Apparently, this fact was used to justify the possibility of observing radio emission from almost horizontal showers [66]. It is known that a long conductor hung at several meters above the ground and loaded at one end by an active resistance of about 600 – 800 Ωm (the Beverage antenna [46]) has a narrow directivity diagram. In the traveling wave regime the major lobe makes an angle with the horizon whose value depends on the conductor's length. The authors of [66] argue that such an antenna of 700 m length at a height of 7 m will effectively register almost horizontal showers from high-energy primary particles.

The papers by the groups from MSU and KSU [56 – 62, 65, 66] constitute only several percent of all papers published since 1965. However, they contain the main results and the directions of studies during this time period for meter and decimeter radio wavelengths.

We should also note the most interesting experimental work of the series of studies carried out on the Havery Park setup (see [67 – 77] for the main results).

Paper [71] is interesting from the point of view of the method used, in which the authors report the observation of radio emission from broad air showers with energy $W_0 \approx 10^{19}$ eV at frequencies 2 and 408 MHz. In the high frequency range, a radio astronomy antenna was employed, while at the medium wavelengths an antenna with capacity impedance was utilized. This was a vertical conductor 1 m in length, on the upper end of which four horizontal conductors 1.5 in length were attached. As a whole, the construction is reminiscent of an open umbrella. The distance to the shower axis was 300 m. Leaving aside many details of the methods of the measurements and calculations, here we reproduce some final results.

The rms radio noise level was around 10^{-3} V and increased by 5% in registering radio emission. Using the relation between the rms amplitude of radio noise A_n, the signal A_s, and the total output amplitude A_t:

$$A_t^2 = A_n^2 + A_s^2 ,$$

the authors [71] estimated the radiation field strength to be ~ 300 μV m^{-1} MHz^{-1}. At the 408 MHz frequency, no increase in noise was discovered and the upper limit of the radio emission field strength was given to be 0.2 μV m^{-1} MHz^{-1}. The main result of this work consists not so much in establishing the fact of the absence of radio emission at high frequencies, as in discovering an intense emission at medium wavelengths. This is one of the first indications of a previously unknown phenomenon.

The concluding paper of this series provides data on the spatial distribution of the radio emission intensity from almost vertical showers with $W_0 \geqslant 2 \times 10^{17}$ eV at frequencies of 60 MHz. The measurements at a distance from 100 to 200 m reveal a radiation field intensity decrease by about an order of magnitude.

In addition, a statistical analysis of a large number of events pointed to a weak dependence of the field strength on the shower energy in the range $2 \times 10^{17} \leqslant W_0 \leqslant 20 \times 10^{17}$ eV at distances 110 m and 230 m from the axis. For virtually all the events the field strength did not exceed 2 μV m^{-1} MHz^{-1}.

At the frequency 1.8 MHz, a multi-vibrator antenna with the suspension height $\lambda/10$ and $\Delta\nu = 200$ kHz was employed. Over an observation period of eight weeks no significant excess above radio noise was found. The authors conclude that the radio emission field strength in this range is on average 0.6 μV m^{-1} MHz^{-1}, which deviates significantly from the earlier results.

To study radio emission, a group of Indian scientists from the university of Guvahati utilized the method of searching for amplitude-frequency correlation between radio pulses associated with a broad air shower. A substantial number of the works cited here [78–94] relate to the low-frequency range. This change in the direction of studies seems to have been natural, as by the end of the 1970s the very limited possibility of using the radio method for radio wavelengths of meter range became obvious. The structure of the experimental setup used at the university of Guvahati did not vary significantly from the typical one. The particle detector was comprised of a system of three Geiger–Muller counters and was designed to generate a master-signal from showers with $W_0 \geqslant 2 \times 10^{16}$ eV. In the high-frequency radio channels of the setup ($\nu > 80$ MHz) a triple-section antenna of 'wave channel' type (the Uda–Yagi antenna) was utilized. In the frequency range $30 \leqslant \nu \leqslant 80$ MHz simple antennas that included one half-wave vibrator were used [82, 84]. The selection of events was made by the oscillograph scan scale. A radio pulse was considered as true, if in triggering the oscillograph by a master-signal, it proved to be in the time interval on the sweep scale known beforehand and showed a sharp frontal shape.

For example, in [84] to assess the relation between radio pulses in one event, the correlation coefficient r for a set of n events was used:

$$r = \frac{\sum_{i=1}^{n}(x_i - \bar{x})(y_i - \bar{y})}{\sqrt{\sum_{i=1}^{n}(x_i - \bar{x})^2 \sum_{i=1}^{n}(y_i - \bar{y})^2}} ,$$

where x_i and y_i are amplitudes in the 60 and 80 MHz range, respectively, and $\bar{x}$ and $\bar{y}$ are their mean values. The value of r found in [84] was +0.68. On this basis the conclusion was drawn that pulses registered simultaneously in different frequency ranges have a common origin.

In [83, 85] the correlation between optical Cherenkov pulses and radio pulses at frequencies 60, 80, and 110 MHz was studied. The correlation coefficients were found to be −0.08, −0.093, and −0.11, respectively. The authors concludes that due to insignificant correlation between optical pulses and radio pulses their nature must be different. For example, since it is well known that optical shower emission is due to the Cherenkov mechanism, there is a high probability for the radio emission to have a geomagnetic nature [7].

Papers [81, 86] provide data on the mean field strength at frequencies 44, 60, and 80 MHz, as well as data from other papers [95, 76, 96] for a distance from the shower axis of less than 50 m. Experimental results indicate that the coherence decreases as the frequency increases. The authors argue that the contradictory results of some papers are due to large experimental errors.

The correlation between amplitudes in the broad frequency range at 60, 80, 110, and 220 MHz was studied in [89]. The results point to a strong correlation between pulses at 60 and 80 MHz. A lack of correlation was established for frequencies 60 and 110 MHz, as well as for 60 and 220 MHz. The authors believe that this fact can be explained by different radio emission mechanisms at high and low frequencies.

The same conclusion is obtained in paper [81] for frequency pairs (9; 60), (9; 220), and (60; 220) MHz, the correlation coefficients for which are found to be +0.38, −0.69, and −0.31, respectively. In [88] an attempt is made to explain the results of these experiments by comparing theoretical estimates of the radiation fields produced by a thin disk of nuclear-active particles (mainly protons) and a disk of excess electrons of a broad air shower. The calculations made for distances 40 and 200 m from the shower axis show that the radiation field strength ratio for electrons and protons, i.e. E_e/E_p, is at least 10 at low frequencies (2 MHz) and decreases to 5 at high (220 MHz) frequencies. In other words, the intensity of radio emission of the nuclear-active component is insufficient to be the dominating mechanism at high frequencies (> 800 MHz).

Paper [93] formulates the main conclusions of earlier results. The authors argue that to uncover the nature of radio emission, more sophisticated equipment is in order.

We can cite several papers in which both the phenomenon of radio emission from a broad air shower was studied and the possibility of cosmic ray detection using this emission was discussed. This problem is treated differently in [97, 98] and in [99]. The experimental technique and its conditions in [97, 98]

differed significantly from those considered earlier. The particle detector was set at a height of 5200 m above sea level near the magnetic equator (Chacaltaya, Bolivia). The detector not only generated the master-signal but also detected the air shower direction, the distance of the setup center from the shower axis, and the number of particles in the shower. To register radio pulses, seven long-period antennas were used with the passband 55–88 MHz and an E–W polarization. Preliminary studies [97] indicated that just such a polarization of the field dominates. The angular size of the major lobe of the beam diagram at the 3 dB level was $75 \times 110^\circ$. In accordance with the conclusions [97], it was oriented at an angle of 45° with the vertical in the West direction. All antennas were set at a distance of 50 m from the setup center. The duration of the radio pulse front caused by an air shower did not exceed several nanoseconds. So the analysis of the delay time of signals for each antenna allowed the determination of the shower arrival direction. Using the results of the experiment, the authors [97, 98] intended to answer the following questions:

1. Will radio pulses from air showers be discernible against the radio noise background?

2. Will the fraction of showers detected by the radio method be sufficiently large?

3. Will it be possible to determine the shower axis direction?

4. Does this method allow the determination of the shower particle number?

During several months 97 showers were detected with radio pulse amplitudes more than two times higher than the rms noise level. An event was counted provided that radio pulses of that amplitude were registered by at least three antennas. Analysis of showers with particle numbers from 10^7 to 10^9 gave positive answers to the first three questions.

Theoretical estimates in paper [99] justify the possibility of cosmic ray detection using a radio component of emission from a broad air shower with energy $W_0 \geqslant 10^{19}$ eV by analyzing radio waves reflected from the conducting Earth's surface. The authors [99] argue that in this case quite appreciable event rates and signal amplitudes can be achieved.

Cosmic ray detection is the process in which their energy, direction of motion, and composition are determined. The first two characteristics can be found with good accuracy using radiation detectors — scintillation counters or Geiger–Muller counters. No well-elaborated method exists to find the third characteristic.

Paper [100] was the first to try to determine the cosmic ray primary composition using the characteristics of radio emission from broad air showers. This relation seems to the authors of [100] quite natural since the depth at which the shower reaches maximum depends on the primary particle mass. This in turn affects the radio emission parameters. Clearly, if the radiation field is formed by an extended source (in this case, by the shower disk), the transverse distribution of the radiation intensity on the Earth's surface directly depends on the distance to the source. Such a dependence is caused by interference. Moreover, the character of the radiation field transverse distribution depends on the observation wavelength. At a given distance from the disk and the ground (which for a specific shower energy, in the authors' opinion, depends only on the mass of the nucleus) and a given wavelength, the field distribution can be unambiguously predicted.

The particle detector used six scintillation counters each 1 m^2 in area. Four counters were located at the corners of a square with a 116 m diagonal, the other two at the square's center.

The registration of radio pulses accompanying the air shower was made in four frequency ranges: 46, 60, 65, and 110 MHz with radio passband widths from 1.5 to 2.5 MHz depending on the range. The construction of antennas involved crossed vibrators with N–S and W–E polarizations. Each of them had an individual feeder and amplifier. One antenna consisted of two similarly oriented vibrators with a suspension height of $\lambda/4$. In the center of the experimental setup three antennas tuned for the range 46, 65, and 110 MHz were mounted. Away from the center (but inside the square) three other antennas working at the frequency of 60 MHz were installed. For each event, the ordinary detector determined the following characteristics:

(1) the shower parameters, i.e. the angle θ between the axis and the vertical, $\rho(r)$ — the particle density at a fixed distance from the axis, α — the angle the shower axis makes with the geomagnetic field vector strength, N — the shower particle number;

(2) the shortest distance from the shower axis to the antenna (four values in total);

(3) the experimental ratio $E_v(\mathrm{E-W})/E_v(\mathrm{N-S})$ for each frequency;

(4) the theoretical ratio $E_v(\mathrm{E-W})/E_v(\mathrm{N-S})$ for two possible emission mechanisms – geomagnetic and Cherenkov;

(5) the radiation field strength.

Based on the results obtained, the following conclusions are made:

1. No notable discrepancy between experimental estimates of the radio emission characteristics and theoretically predicted values is found.

2. Despite the absence of a contradiction with the theory, the frequency spectrum and the transverse distribution can not provide information on the primary cosmic ray composition.

3. The reason for this, in the authors' opinion, could be the insufficient distance of antennas from the setup center and large measurement errors.

To conclude the review, we should present the results of the discussion between the groups of researchers in Moscow, Havery Park, and Bologna [101] on the electric field strength of radio emission from air showers and possible reasons for experimental data dispersion.

In spite of general agreement as to the generation mechanism, the experimenters disagree on estimate of the absolute intensity of radio emission from a shower of given energy. At the International Cosmic-Ray conference in Munich, the Moscow group [102] and the Havera Park group [76] pointed to typical strength values differing by 6 ± 2 times (3.4 and 0.6 μV m^{-1} MHz, respectively). In part, this difference, the authors believe, is due to an uncertainty in establishing the relation between the shower energies as measured by the number of muons N_μ (Moscow) and energies as measured by the parameter ρ_{500} (Havera Park).

Radio pulses accompanying broad air showers notably exceed the radio background for particle energies $W_0 \geqslant 10^{17}$ eV at a distance of ~ 100 m from the shower axis. Assuming the geomagnetic radio emission mechanism to dominate in the range of meter radio waves, the field strength should be characterized by the parameter (the

normalised field strength)

$$E_v^N = \frac{E_v}{E_p \sin\alpha},$$

where E_v is the measured field strength, $\mu V\,m^{-1}\,MHz^{-1}$, E_p is the shower energy, 10^{17} eV, and α is the angle the shower axis makes with the geomagnetic field in degrees (Table 3). In Havera Park, the normalization $E_p = 10^{17}$ eV is made using the parameter ρ_{500} (the particle density at a distance of 500 m from the axis). The field strength 3–4 $\mu V\,m^{-1}\,MHz^{-1}$, given by the Moscow group, is obtained assuming a shower with energy 10^{17} eV to contain 1.7×10^5 muons with an energy larger than 10^{10} eV. The characteristic field strength, estimated by the Bologna group [103–105], is 12 $\mu V\,m^{-1}\,MHz^{-1}$. But data from this group can not be normalised using the Moscow group method, since these data represent the mean of the measured values $E_v/\sin\alpha$ for showers which contain from 10^6 to 3×10^7 electrons. The mean energy corresponding to this number of particles is $\sim 10^{17}$ eV. However, thus determined it has a high error due to significant fluctuations of the electron number in showers generated by the same primary energy E_p.

Table 3.

Year	Research group	E_v^N, $\mu V\,m^{-1}\,MHz^{-1}$	References
1971	in Havery Park	5–10	[64]
1973		~ 1	[75]
1975		~ 0.6	[76]
1975	in Moscow	3.4	[102]
1976	in Bologna	15	[105]

In addition, the authors believe that a possible reason for the discrepancy could also be the different calibration methods for the registering equipment. For example, this could be for the following reasons:

1. Parameters of antennas were calculated, not measured. The antenna amplification coefficients could differ significantly from theoretical values for a poor quality of construction.

2. The presence of nearby radio receiver centers decreases the amplification coefficient of radio receivers due to violation of the linear regime of amplification cascades or the detector's working regime.

3. The calibration of antennas using galactic radio noise produces a significant error since the equivalent temperature of the celestial sphere at the frequency 60 MHz can vary by an order of magnitude depending on the sidereal time and the orientation of the antennas.

Thus, despite a significant dispersion of experimental values of the normalised field strength, the authors argue that a shower with geomagnetic radiation and particle energy 10^{17} eV would produce a field at a distance of ~ 100 m with a strength on the order of 'several $\mu V\,m^{-1}\,MHz^{-1}$'.

4. Experimental studies of radio emission from air showers at low and medium frequencies

The field strength of radio emission from an air shower for the Cherenkov [6, 19] and geomagnetic [7] radiation mechanisms is proportional to the frequency. This implies, for example, that the characteristic field strength at the frequency 1 MHz must be, according to [101], ~ 0.1 $\mu V\,m^{-1}\,MHz^{-1}$. However, earlier studies [71, 106–108] already revealed that the experimentally measured spectral field strength at low frequencies is several orders of magnitude larger than the theoretical values found in [6, 7, 19]. The low-frequency range is very inconvenient for the study of radio emission due to the high level of atmospheric noise. So the experiments [71] measured not individual radio pulses, but the total rms amplitude of the radio noise (see Section 3).

An attempt to establish the nature of the low-frequency emission was made in paper [109]. The author evaluated the upper limit of the radiation field strength at 5 MHz produced by all charged particles of the shower for known radio emission mechanisms with and without taking into account the Earth's magnetic field. Despite unrealistic assumptions that increase the theoretical intensity estimate (such as lengthening of the particle tracks to infinity, ignoring the disk thickness, etc.), the spectral field strength estimate was less than 100 $\mu V\,m^{-1}\,MHz^{-1}$ for a shower with $W_0 = 10^{17}$ eV. This suggests that either experimental estimates are incorrect, or there is a radio emission mechanism of unknown nature.

It should be noted that the mechanism of radio emission from the shower (by electrons and positrons) due to bending of trajectories in the Earth's magnetic field was discussed much earlier in [110], where the possibility of using a radio detector in addition to an optical detector of particles was discussed. In [100], the maximum radio emission is estimated to be ~ 2 MHz. The author concludes that there is a possibility of significantly increasing the efficiency of this method for high-energy particles. Such a combination of two setups allows the registration of both almost vertical and horizontal showers.

The measurement of the field strength at the frequency 2 MHz was performed at a good experimental level in [107]. A distinctive feature of the experiment was the utilization of a radio astronomy antenna with a vertical directivity diagram at the frequency 1.98 MHz. It comprised 178 half-wave vibrators and had an angular size of the main maximum of about 8° at half-height. The passband of the radio receiver was selected to 70 kHz. The triggering of the setup was performed by a pulse produced by the Cherenkov optical detector consisting of an aluminum spherical mirror 112 cm in diameter and photo multipliers mounted in the focus of the mirror.

Statistical processing of the results revealed that radio signals registered by the detector originate in broad air showers. The mean field strength for 100 showers observed with energy $W_0 = 2 \times 10^{14}$ eV was 1 $\mu V\,m^{-1}\,MHz^{-1}$. Since for the coherent mechanisms the field strength is proportional to the primary energy, the extrapolation in the high-frequency region yields 500 $\mu V\,m^{-1}\,MHz^{-1}$ for $W_0 = 10^{17}$ eV, which is confirmed by the results [71].

The theory of antennas shows that a vibrator of length 0.5λ can be used as an emitter of the third harmonic, with the resistor at its terminals staying active and virtually unchanged. This property of vibrators was employed to measure the field strength of radio emission in the frequency range 6 MHz [112] using an antenna with a main resonance frequency of 2 MHz [107]. In addition, it proved possible to estimate the character of polarization of the emission. For this one half of the 178 vibrators were oriented in the E–W direction, while the other half was oriented in the N–S direction. Each of them operated as an independent antenna.

The measurements showed that the mean pulse amplitudes of the (W – E) and (N – S) antennas were 5 and 2.2 μV, respectively. The authors of [112] argue that the comparatively large amplitude of the (N – S) antenna indicates a significant contribution due to a mechanism unrelated to the Earth's magnetic field. The field strength normalised to $\sin(\widehat{\mathbf{vH}})$ and to the energy $W_0 = 10^{17}$ eV is estimated to be 140 ± 50 μV m^{-1} MHz^{-1}. Using data [71, 106 – 108] and the results of their work, the authors concluded that there was a linear decrease of the field strength in the frequency range from 2 to 22 MHz.

The same decreasing frequency dependence of the spectral field component is reported in paper [87] cited above. The group of scientists of the University of Guvahati (India), who studied the radio emission mechanism from air showers in a broad frequency range over many years, arrived at the conclusion that there is satisfactory agreement between experimental results and theory in the meter wavelength range (44 – 220 MHz). At decameter ($\lambda > 30$ m) and longer wavelengths, experimental data deviates from theory (Table 4). The values of the field strength determined experimentally by this group at different frequencies listed in this table are approximately consistent with data from other studies.

Table 4.

Frequency, MHz	Field strength, μV m^{-1} MHz^{-1}	
	Experiment	Theory
2	1556 ± 621	—
9	525 ± 57	—
44	13.3 ± 0.7	16.8
60	12.25 ± 0.56	12.25
80	7.7 ± 0.6	8.4
110	7.1 ± 0.8	7.35
220	1.14 ± 0.34	3.15

Somewhat later, an attempt [94] was made to modify the geomagnetic mechanism hypothesis [7]. However, numerical calculations did not produce the desirable result. Later on, this group, as well as some others, looked to solve this issue by invoking the transition radiation mechanism [114 – 115]. However, the calculation methods used, in the opinion of the author of this review, were not fully adequate for the purpose pursued.

The above conclusions could give the impression that the effect of the spectral field component growth with a decrease in frequency is reproducible and commonly accepted. However, this is not the case. In the paper [106] mentioned above, groups from the University of Adelaide and the Polytechnical Institute of Hatfield (England) studied radio emission intensity many times at low [116] and medium [108] frequencies. The results given below for three frequencies are the generalization of these works.

The input of radio receivers was attached to an antenna consisting of two crossed half-wave vibrators with a resonance frequency 3.6 MHz and passband 0.4 MHz. The estimate of the shower energy and the master-signal generation were performed by a scintillation particle detector. The mean field strength at this frequency was less than 0.7 μV m^{-1} MHz^{-1} for showers with particle number 10^6.

A direct amplification radio receiver with a 700 kHz passband was attached to the output of an antenna that included four half-wave dipoles with the resonance frequency 2 MHz. As in the previous case, an upper limit of the field strength of 0.5 μV m^{-1} MHz^{-1} was estimated by the rms noise amplitude. No explicit signal was detected in this frequency range.

The antenna for the 100 kHz range consisted of one copper conductor 90 m in length suspended 3 m above the ground. A radio receiver with an autonomous power supply and 80 kHz passband was set immediately below the antenna. No definite results were obtained in this frequency range. The signal-to-noise ratio varied from very large to zero values with a period of several days. The authors concluded that data from measurements at 2 and 3.6 MHz, although being inconsistent with previous measurements, do not contradict theoretical calculations [7]. No assumptions as to the 100 kHz range were made.

It should be stressed again that measurements at such a low frequency under the conditions described in that paper are meaningless. Clearly, a conductor 90 m in length was in the quasi-static field and not in the radiation field, and it can not directly serve as an antenna.

In the second half of the 1980s, studies of radio emission at meter and decameter wavelengths practically entirely shifted toward low and medium frequencies. A significant number of these studies were carried out by Japanese researchers. One of their first publications [117] was connected to the discussion initiated by the report [118] at the 18th International Conference on Cosmic Rays on the possibility of the detection of very high energy air showers at large distances from their axes.

A feature of the experimental study [117] was the significant distance of the receiving antennas from the shower axis ($\sim 1-2$ km). The Akeno installation with a working area of 20 km^2 was used as the particle detector. Moreover, here antennas with vertical polarization were used for the first time. This apparently implied that the authors did not count on the efficiency of the geomagnetic mechanism. One of the antennas (so-called spherical) was essentially a loaded vertical vibrator. A metallic hemisphere 0.5 m in diameter was attached to the upper end of a conductor 10 m in length. The capacity of such an antenna was ~ 100 pF. The second antenna had the same construction as the first, but did not have the loading capacity in the form of the hemisphere. The preamplifier with an input capacity of 100 pF and an input resistance of 20 MΩ was attached directly to the bottom part of the conductor. The observations were made at frequencies 50 kHz, 170 kHz, and 1 MHz by radio receivers with a ±71 kHz passband at the 50 dB level. The number of particles in the showers measured by the Akeno detector fell within the interval $10^7 - 2 \times 10^{10}$.

Analysis of the measurements showed that the radio pulse field strength is at least 10 – 100 times larger than expected from geoelectric mechanisms. The authors of [117] argue that the most likely radiation mechanism is the acceleration of ionization electrons in the atmospheric electric field. The absolute field strengths at a distance of ~ 2 km are several millivolts per meter. It should be noted that there is a quite different explanation for the results of this experiment (see [41] for more detail).

As a reaction to discussion [118], theoretical paper [119] appeared among others, where the author compared the field strengths produced by the geomagnetic mechanism and by transition radiation at frequencies 10 kHz, 100 kHz, and 1 MHz. The author of this paper does not describe the method of his calculations. So we restrict ourselves to considering a

short example: the calculated strength is reported to be 100 μV m^{-1} MHz^{-1} at a distance of 1 km from the axis at the 1 MHz frequency for a shower with energy $W_0 = 10^{20}$ eV. This result fully coincides with data on the field strength from paper [42]. The spectral intensity maximum is estimated by the author to be in the frequency range from 1 to 10 MHz. It should be noted that considering realistic observational conditions for the transition radiation, i.e. the position of the observer is not above the shower but on the ground plane, this estimate of the spectral intensity maximum need to be made more precise. See [42] for more detail.

A further elaboration of studies in this direction is presented in [26]. At the Akeno detector showers with particle numbers from 10^9 to 1.5×10^{10} were selected. The detection of radio pulses was performed using a vertical antenna 10 m in height attached to a high-Ohmic amplifier (see above). After recording, radio signals were subjected to an amplitude-frequency analysis in the range from 26 to 300 kHz with the aim of excluding components outside the signal spectrum. The observed signals were discovered to be unipolar and to have a duration of 5 μs. The field strength varies inversely proportionally to the distance from the shower axis to the antenna. Its value at a distance of 2–2.5 km is 40 μV m^{-1} MHz^{-1} for a shower with particle number 10^9. The authors of [26] came to the conclusion that the radiation due to excess electron collisions with the ground is the most likely reason for radio emission.

Knowledge of the dependence of the field strength on the distance between the shower axis and the antenna facilitates the uncovering of the nature of the electromagnetic pulse. This relation was examined in [121]. The technical equipment was largely the same as described in earlier papers (see above). The useful signal was singled out from the noise by computers. To do this the signal recorded with radio noises was presented by its amplitude-frequency characteristics. In this spectrum, the noise component can be easily distinguished by sharp peaks on the diagram. After its subtraction, the inverse transformation was done. To get the field strength as a function of the distance, the results of the measurements were normalised to a shower with 10^8 particles, i.e. the strength was multiplied by the ratio $10^8/N_e$, where N_e is the shower particle number. Such a dependence has the form

$$E = 10^{4\pm0.4} R^{-(0.7\pm0.33)} \text{ μW m}^{-1} \text{ Hz}^{-1}.$$

The data obtained allowed the authors to conclude that the nature of the emission observed by them can not be related to the mechanism of transition radiation from excess shower electrons, since the field strength measured is two orders of magnitude higher than theoretical estimates.

Using the same experimental equipment, the group [27] observed giant electromagnetic pulses from showers with the numbers of particles in excess of 10^5. The duration of such pulses was found to lie within the 10–15 μs range, and the field strength was about 50 μV m^{-1}. The authors argue that they could be due to an interior cloud discharge. In the critical field strength range $\sim 10^6$ W m^{-1}, tracks of charged particles of a broad air shower could initiate an electric discharge or a powerful electron avalanche — the precursor of the electric break-down [122]. In both cases, strong electromagnetic inductions are possible.

The group from the Tokyo Polytechnical Institute estimated the field strength due to the breaking of shower electrons by ionization losses. The strength in this model is a function of R — the distance to the observation point, θ — the zenith angle, and ψ — the angle between the line connecting the shower center with the antenna and the shower axis projection on the ground. The results of calculations were tested on the Akeno detector. To register radio pulses, an antenna with vertical polarization was utilized. The authors believe that the measurements of the field strength confirm the emission model predictions.

The particle detector in Yakutsk, like the Akeno detector, is one of the largest in the world. Under highly unstable atmospheric conditions, groups of researchers from the Yakutsk Institute for Cosmophysical Studies and the Moscow and Grozny State Universities studied the low-frequency (1–100 kHz) radio emission from broad air showers [28]. The electric signal induced in the two-meter vertical antenna arrived at the oscillograph input through a cathode repeater, a passband filter, and the delay line. The time-base block was triggered by a master-signal from the particle detector. The series of experiments included 5000 records obtained in Yakutsk and 800 records obtained in Grozny. The probability of registration unrelated to the shower was estimated by the authors to be $\sim 10^{-3}$. The mean shower energy according to the Grozny and Yakutsk experiments was $W_0 = 10^{16}$ eV and $W_0 = 10^{17}$ eV, respectively. The authors of [28] noticed a very high field strength (~ 300 mV m^{-1}) in the frequency range under study and argue that the radio emission has a geoelectric origin.

Thus this brief review of the results of studies on the nature of radio emission in the low and medium frequency range indicates that by 1985–1990, the range of problems was clearly recognized, stimulating further searches for the radio emission mechanisms. In addition, these studies gave some hope for the possibility of developing a high energy cosmic ray radio detection method.

5. On the prospects of cosmic ray radio detection methods

Although the above review of experimental studies is not exhaustive, it encompasses the main results of studies of the radio emission origin over a broad wavelength range. Let us briefly enumerate the main conclusions from the above studies.

Meter wavelength range:

(a) Radiation mechanism can not be definitely determined, however the relation to the Earth's magnetic field is obvious;

(b) Small signal-to-noise ratio;

(c) Narrow spatial emission directivity diagram ($\sim 2-3^\circ$);

(d) No unique signal amplitude dependence on the shower particle number.

As mentioned above, the traditional detection method of cosmic rays with energy $W_0 \leqslant 10^{19}$ eV is almost fully adequate to the purposes pursued. If this method is somehow restricted in this energy range, it is presently unclear how the radio detection method could overcome this shortcoming. In other words, the possibility of development in this direction does not appear to be very promising, at least for now.

Medium and long wavelength range:

(a) Radio emission mechanism is not definitely known;

(b) Spectral field strength is two to three orders of magnitude higher than in the meter wavelength range;

(c) High level of atmospheric and industrial noise makes the method practically unrealizable;

(d) Maximum distance of the observer from the shower axis in these experiments (2 – 3 km) is an order of magnitude higher than in the meter wavelength range.

Apparently, in those cases where observations were made in the wave and not in the Coulomb zone, the radio emission was connected to transition radiation of the shower disk polarized in the Earth's magnetic field (see Section 2.8). In this case, as found, for example, in [9], at a distance of 10 km the field strength is $E_\omega = 60$ μV m^{-1} MHz^{-1} for a particle with $W_0 = 10^{20}$ eV. Since $E_\omega \sim W_0/R_0$, it is easy to find that at a distance of 2 km for $W_0 = 10^{19}$ eV the field strength is 30 μV m^{-1} MHz^{-1}. This is likely to be sufficient to explain the results of the observations (see [26, 118 – 122, 124]).

The need to study high-energy cosmic rays led to the idea of registration of radio signals from a cascade shower induced by a primary cosmic ray particle on the Moon's surface. As the lunar soil has a density three orders of magnitude higher than in the Earth's atmosphere, then, as was noted earlier [6, 125], the radiation intensity in such a medium is much higher than in the normal atmosphere. This idea is also attractive because the area of the visible lunar surface (10^7 km^2) is 5 to 6 orders of magnitude larger than the working area of traditional detectors. This means that the probability of registration of a cosmic ray particle increases by the same amount.

It is possible to register a radio signal from a cascade in the lunar soil on the Earth's surface using an artificial satellite of the Moon or using a radio telescope (i.e. by radio astronomy methods). Such a possibility was first justified in [126], in which the authors made use of the earlier estimate [50] of the energy W of the coherent Cherenkov radio emission from a cascade shower in a dense medium. Inside the entire wavelength range, $W \approx 10^{-10}\ (W_0/10^{14})^2$ erg, where W_0 is the cascade energy in electron-volts. On this basis, the authors believe that modern radio telescopes are capable of registering cascades triggered by high-energy neutrinos ($10^{20} - 10^{22}$ eV) interacting with the soil material of the Moon's visible side.

The radiation spectrum at frequencies $\nu \leqslant \nu_{\max} \approx 1$ GHz is proportional to the frequency. So the radio pulse energy radiated over time $\Delta t = 10^{-8}$ s within the cone subtending the solid angle $\Omega = 0.5$ ster, would generate for the terrestrial observer the flux

$$S_{\rm pls} = 2\nu W(\nu_{\max}^2 \Omega R_{\rm me} \Delta t)^{-1} = 3\times 10^{23} \nu_0 W_{20}\ ({\rm W\,m^{-2}\,Hz^{-1}})\,,$$

where $R_{\rm me}$ is the distance from the Earth to the Moon, $\nu_0 = \nu/10^9$ and $W_{20} = W_0\,({\rm eV})/10^{20}$. A comparison of this flux with the sensitivity $S_{\rm eff} = 2kT/A_{\rm eff}\,\Delta t$ of radio telescopes with an effective antenna area of $A_{\rm eff} \sim 10^4$ m^2 indicates that for certain detection modes (see [126] for more detail), cascades produced by primaries with $W_0 \geqslant 10^{20}$ eV could in principle be detected from the Earth.

In addition, the authors of [126] found that in the visible lunar soil layer of thickness ~ 5 m, about 10^5 observable neutrino events should occur per year, which would allow testing of some models of the Universe. The radio emission from cascades triggered by protons (nuclei) can emanate from the lunar soil due to scattering processes. Of special interest could be interaction of cosmic hadrons (or γ-quanta) with energy $W_0 \geqslant 10^{20}$ eV with the Moon's surface. In this case, unlike the neutrino processes, radio pulses should be observed from cascades only on the lunar disk edge.

The idea of the radio cosmic ray detection method seems very attractive. In [128], calculations of the radio detector threshold sensitivity were performed as a function of the radio telescope characteristics. The minimum energy of the electromagnetic cascade is found to be

$$E_0 \cong 2.7\times 10^{11} \sqrt{\frac{T(s/n)}{A_{\rm eff}}}\ \frac{1 + 2.36\times 10^{-7}\nu}{\nu\sqrt{\Delta\nu}}\,,$$

where E_0 is expressed in Tera-electron-volts, ν is the frequency in MHz, $A_{\rm eff}$ is the effective area of the antenna in m^2, s/n is the rms signal-to-noise ratio, and T is the noise temperature of the antenna. This result makes allowance for the change in the angular width of directivity diagram due to the LPM-effect (Landau – Pomeranchuk – Migdal) caused by collective interaction of atoms and molecules of the medium with particles of the electromagnetic cascade, which diminishes the effective cross sections of bremsstrahlung and electron – positron pair creation. For the lunar soil, this effect becomes significant at energies above 0.5×10^{15} eV.

The following data was used in the calculations: the lunar soil density 3 g cm^{-3}, the refractive index $n = 1.8$, the radiation length unit $t_0 = 22.6$ g cm^{-2}, the critical energy 40 MeV, the Moliere radius 11.8 g cm^{-2}, and the Cherenkov angle 56°. The radiation is found to stay coherent up to frequencies of ~ 3 GHz. If the cascade is produced by a heavy primary, the associated radio pulse can be observed only in a narrow ring-like layer on the Moon's surface whose size is determined by the refractive index of the soil. This implies that only neutrino-triggered radio pulses can originate in the central part of the visible lunar surface. Paper [128] also contains the results of calculations of the neutrino event rate depending on the radio telescope parameters.

The author argues that one possible way of developing the cosmic ray radio detection method should be connected to the shower emission beam features at wavelengths significantly exceeding its longitudinal size. It is known that there are no narrow-beamed emitters with a size much smaller than the emission wavelength. This makes it possible to determine in a relatively simple way the shower axis orientation with respect to the vibrators of mutually perpendicular antennas (see below for more detail).

The author believes that significant progress in the radio detection method can be achieved provided that [131]:

(1) the energy range under study is above $W_0 = 10^{20}$ eV;

(2) the Moon's surface is taken as the working detector area;

(3) the radio pulse detectors with antennas are located on an artificial satellite of the Moon.

Apparently, there are other points of view on the possible ways of developing high-energy cosmic ray detection principles. However, the author of the present paper argues that the discussed method is most promising, which will be justified below. It should be noted that to this end, as the author believes, the radio emission mechanism caused by the current of the shower δ-electrons is most appropriate (see Section 2.5). In this case, neither magnetic field nor atmosphere is required. The electron – photon cascade generated by a high-energy particle would develop underneath the lunar surface. Due to the absence of water, the lunar surface's electric conductivity is close to zero, so it virtually will not absorb electromagnetic waves along a path of the order of a wavelength.

As industrial and atmospheric noise are naturally absent on the Moon, the lunar surface is a very favorable place for the task pursued with regard to noise protection.

The cosmic ray flux intensity is known to decrease with energy according to the power law:

$$J(> W_0) = AW^{-\gamma}.$$

If this relation holds as the energy increases ($\gamma \approx 2.7$ for $W_0 = 10^{19} - 10^{23}$ eV), we can hope that the event rate will be quite acceptable for the studies.

The degree of influence of the Landau–Pomeranchuk-Migdal effect [120] on the longitudinal size of the electromagnetic cascade is essential for elaborating the radio detection method, the essence of which will be given below. The calculation of the cascade function for a particle with energy $W_0 = 10^{21}$ eV producing a shower in a medium with density $\sim 10^3$ kg m^{-3}, showed [129, 130] that the longitudinal size of such a shower is about one and a half orders of magnitude larger than the air shower. Should this be the case, the radio emission spectral distribution will drastically change: the spectral density energy maximum will shift from the short to the medium wavelength range. Presently, however, this effect is rather hypothetical, as no experimental evidence has been found. Moreover, it will not principally alter the method under consideration, so we will not consider the LPM effect for a while. In any case, the main points will stay unchanged. Only the tactics will change.

According to [10–12], quasi-coherent radio detection is possible for wavelengths $2L < \lambda < \infty$, where L is the longitudinal size of the shower. For the lunar soil $L = 5–10$ m, so at frequencies $\nu \sim 30$ MHz a maximum field strength should be expected. In the same wavelength range, the cosmic radio noise produces less than 3–4 μV m^{-1} MHz^{-1} [43, 44].

Now we need to show that the radiation field strength from the electron–photon cascade caused by a primary particle with energy $10^{21} - 10^{23}$ eV on the Moon's surface will be sufficient for reliable registration of the associated radio pulse. In this connection we can refer to the earlier papers [10–12], in which the field spectral component corresponding to the δ-electron current for a particle with energy $W_0 = 10^{20}$ eV is found to be $E > 50$ μV m^{-1} MHz^{-1} at a distance of 10 km from the shower axis. As the field strength is proportional to W_0/R, this component will exceed 250 μV m^{-1} MHz^{-1} for an orbit with altitude ~ 2000 km. In the absence of industrial and atmospheric noise, this value is more than sufficient for reliable radio pulse registration [15]. Moreover, such a high orbit would allow about 1/3 of the lunar surface to be observed. To register particles of smaller energy, for example with $W_0 = 10^{21}$ eV, the height of the orbit can be reduced to 100 km. Then the field strength $E > 50$ μV m^{-1} MHz^{-1} and the observational area will be about 10^6 km^2.

From the above one can imagine the following main constituents of a new generation detector: it should be on an artificial satellite $(1–2)R_m$ above the Moon, with a radio receiver and simple antenna (a half-wavelength vibrator) mounted. Such an altitude allows practically half of the Moon's surface to be observed, which ensures a registration rate of about 10 events per year with $W_0 = 10^{23}$ eV (see the note above) provided that the energy spectrum power index remains the same inside the interval $10^{19} - 10^{23}$ eV (i.e. $\gamma \approx 2.7$). The launch of a the detector into lunar orbit is very expensive, so it would be natural to expect this method to yield more information than merely particle detection. The measurement of a radio pulse amplitude by one antenna gives virtually no information on the particle energy (as the distance to the cascade produced by this particle is unknown) or its motion direction. But this data can be obtained by two modules in lunar orbit with radio detectors onboard.

As the lunar soil has zero electric conductivity, the cascade shower polarization mostly depends on its axis location. If the two modules are in orbit and each has an antenna consisting of three mutually perpendicular vibrators, the pulse polarity and amplitude in each of the six vibrators will depend on the relative orientation of the shower axis. This data would suffice to establish the shower coordinate angles and the distance from its axis, and to determine the electromagnetic cascade energy. Let us consider this in more detail [132].

The cascade shower axis is determined by three mutually perpendicular vibrators. It is known that the directivity diagram of an isolated vibrator of length $2a$ is expressed in the form

$$F(\alpha) = \frac{\cos(ma\cos\alpha) - \cos ma}{(1 - \cos ma)\sin\alpha}, \tag{5.1}$$

where $m = 2\pi/\lambda$ and α is the angle between the dipole axis and the line of sight **n** (see, for example, [46]). As a rule, half-wave vibrators are used as simple antennas (and as elements of more complex ones). However, considering the actual detector construction in a lunar orbit, the use of a half-wave vibrator ($a = \lambda/4$) of length about $2a = 5$ m ($\nu = 30$ MHz) could be technically difficult. In such cases one utilizes shortened vibrators with inductances successively included in their circuits to preserve resonance frequency. It is known that such a change does not notably worsen the signal-to-noise ratio if the radio receiver sensitivity is determined by the external noise level. In our situation this is precisely the case as the equivalent temperature of the celestial sphere (~ 10000 K) exceeds the noise temperature of the input circuits of the radio detector (600–800 K) at these frequencies by at least one order of magnitude.

It is easy to make sure that Eqn (5.1) can be replaced by the function $F_1(\alpha) = \sin\alpha$ with an accuracy sufficient for practical purposes. For example, in making the half-wave vibrator 2 times shorter ($a = \lambda/8$), the difference between these beams is less than 2%. So we shall use further the normalised function $F_1(\alpha) = \sin\alpha$ as the spatial directivity diagram of the receiving antenna of the detector. Moreover, we shall take into account, according to [10–12], that the shower emission directivity diagram in the wavelength range $\lambda > L$ (where L is the longitudinal size of the shower) is approximately expressed by the function $F_1(\alpha)$ as well, i.e. the radiation field strength at an arbitrary point is $E = E_0 \sin\alpha$, where α is the angle between the emission direction **n** and the cascade axis. It is also known that the strength vector **E** lies in the plane the shower axis (or the dipole axis if the antenna radiates) makes with the line of sight **n**. Furthermore, in the far zone the field strength always satisfies the condition $\mathbf{E} \perp \mathbf{n}$.

In the author's opinion, to determine the cascade shower axis (and hence the arrival direction of a cosmic ray particle on the lunar orbit), two modules should be present. Each of the modules should be equipped with three identical mutually perpendicular vibrators, signal amplifiers (for each vibrator), measurement devices for the e.m.f. amplitude induced in each of the antennas, as well as a complex of devices for determining the relative module location in the frame connected to the Moon. The modules should be located

within direct visibility, but not too close to each other for the measurement error to be small.

The cascade shower in the lunar soil produced by a ultra-high energy charged particle crossing through its surface would induce the e.m.f. u_{1x}, u_{1y}, u_{1z}, and u_{2x}, u_{2y}, u_{2z} on the terminals of the first and second module antennas, respectively. Clearly (see, e.g., [46]), the e.m.f. can be expressed through the field strength vector E and its directional cosines ϕ, ξ, η. This yields eight equations for the fields $\mathbf{E}_1$ and $\mathbf{E}_2$ in the frame of each module:

$$u_{ix} = \frac{LE_i}{R_i} \sin\alpha_i \cos\phi_i \,,$$
$$u_{iy} = \frac{LE_i}{R_i} \sin\alpha_i \cos\xi_i \,, \quad i = 1, 2 \,,$$
$$u_{iz} = \frac{LE_i}{R_i} \sin\alpha_i \cos\eta_i \,,$$
$$\cos^2\phi_i + \cos^2\xi_i + \cos^2\eta_i = 1 \,, \tag{5.2}$$

where L is the effective length of the antenna, $i = 1, 2$ is the number of the module, R_i is the distance from the module with the number i from the shower axis, α_i is the angle the shower axis makes with the vector $\mathbf{R}_i$.

Let us consider a straight line formed by the intersection of the planes A_1 and A_2 passing through the origin of each module frame. The directional vectors for each plane are taken to be $\mathbf{E}_1$ and $\mathbf{E}_2$, respectively, whose components are proportional to the e.m.f. induced in the corresponding antennas:

$$u_{1x}x_1 + u_{1y}y_1 + u_{1z}z_1 = 0 \,,$$
$$u_{2x}x_2 + u_{2y}y_2 + u_{2z}z_2 = 0 \,. \tag{5.3}$$

Putting a source of light at an arbitrary point on line (5.3), the emission direction toward each of the modules will be perpendicular to $\mathbf{E}_1$ and $\mathbf{E}_2$, respectively, for arbitrary angles α. In other words, the cascade shower (as a point) for a given set of parameters u_{1x}, u_{1y}, u_{1z} and u_{2x}, u_{2y}, u_{2z} can be positioned only on line (5.3). Considering the cascade shower is simultaneously on the surface of the Moon, the intersection of (5.3) with the sphere $x^2 + y^2 + z^2 = R_{\rm m}^2$, where $R_{\rm m}$ is the Moon's radius, uniquely determines its coordinates x_0, y_0, z_0 (Fig. 7). The shower axis, according to the above, must simultaneously lie in the plane of vectors $\mathbf{R}_1$, $\mathbf{E}_1$ and $\mathbf{R}_2$, $\mathbf{E}_2$. So to find its direction, plane A_3 should pass through the first module frame origin $O_1(x_1, y_1, z_1)$, the point x_0, y_0, z_0, and the direction $\mathbf{E}_1$, whereas plane A_4 should be drawn through the second module frame origin $O_2(x_2, y_2, z_2)$, the point x_0, y_0, z_0, and the direction $\mathbf{E}_2$:

$$\begin{vmatrix} x - x_1 & y - y_1 & z - z_1 \\ x_1 - x_0 & y_1 - y_0 & z_1 - z_0 \\ E_{1x} & E_{1y} & E_{1z} \end{vmatrix} = 0 \,,$$
$$\begin{vmatrix} x - x_2 & y - y_2 & z - z_2 \\ x_2 - x_0 & y_2 - y_0 & z_2 - z_0 \\ E_{2x} & E_{2y} & E_{2z} \end{vmatrix} = 0 \,. \tag{5.4}$$

Line (5.4) along which these planes intersect gives the direction of the cascade shower axis.

This method of calculation of the cosmic particle motion direction also allows for the determination of the number N_0 of electrons in the cascade shower maximum. According to [10 – 12], the radio pulse amplitude is expressed as

$$E = BN_0 \frac{\sin\alpha}{R} \,,$$

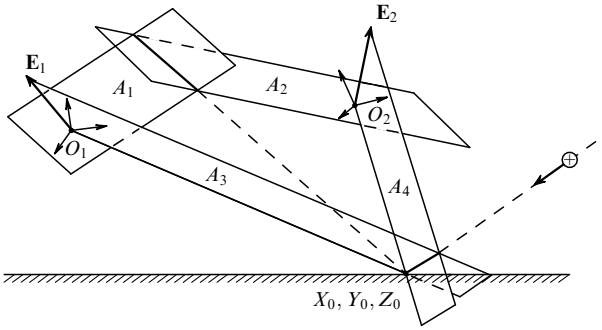

Figure 7. Illustration of the cascade direction determination. The dashed line marks the primary motion direction. O_1 and O_2 are the first and second modules reference frames (other explanations are in the text).

where B depends only on physical constants and is known. So the determination of the directional cosines from Eqn (5.3), as well as of the ratio $\sin\alpha/R$, according to the method under consideration, allows for the unique determination of the number of electrons N_0 in the shower and hence the primary particle energy W_0.

The scheme of determining the cosmic particle motion should be completed as follows. Equations (5.2) for $i = 1, 2$ determine the coordinates E'_{ix}, E'_{iy}, and E'_{iz} of the vector $\mathbf{E}_i$ in the first ($i = 1$) or the second ($i = 2$) module frame. To solve equations (5.3), (5.4), it is necessary to express the projections E'_{ix}, E'_{iy}, and E'_{iz} through the corresponding projections E_{ix}, E_{iy}, and E_{iz} of these vectors in the frame connected to the Moon. This can be performed using the vector transformation matrix in a Cartesian frame rotation. At any time, its elements can be calculated by the orientation determination system of the modules, and this operation is a standard procedure in the space technique.

Thus the above results make the high-energy cosmic ray radio detection method comparable to traditional detection methods. It allows for the determination of the number of particles in the shower and of the primary arrival direction. Moreover, the determination of the nuclear composition can be discussed, as the cascade function depends on the number of nucleons in the nucleus and this dependence affects the spectral energy density distribution.

The testing of the main points of a project always precedes its realization. Is there such a possibility in this case? The answer is yes. It is possible to perform a low-cost experiment without launching a spacecraft [14]. Using the above obtained field strength $E > 50$ μV m^{-1} MHz^{-1} from a cascade with energy $W_0 = 10^{20}$ eV at a distance of $R_0 = 10$ km from the emission source (i.e. the shower), it is easy to estimate that the field strength on the Earth from a shower with energy $W_0 = 10^{23}$ eV on the Moon will be $E_\omega = 50(R_0/R_{\rm me}) \times 10^3 \approx 1$ μV m^{-1} MHz^{-1}, where $R_{\rm me} = 0.4 \times 10^6$ km is the distance to the Moon.

It is interesting to note that within the framework of the δ-electron current model it is easy to evaluate the spectral field component without making complex calculations. In this case the shower propagation in the medium is equivalent to the motion of a short current pulse along a conductor. In estimating the mean current strength, let us use the data on the excess number of electrons in a shower with energy above 20 MeV, i.e. $N_{\rm e} = kN_0$, where $k = 0.1$ according to [6] and N_0 is the total number of particles. Clearly, in this case we somewhat underestimate the field strength. Next we find:

a) the time τ of the longitudinal motion of the shower: $\tau = L/c = 3 \times 10^{-8}$ s, where $L \sim 10$ m is the longitudinal size of the shower;

b) the mean current strength across the path L over time τ:

$$I = \frac{kN_0ec}{L} = 50 \text{ A},$$

where $e = 1.6 \times 10^{-19}$ C is the electron charge;

c) the current amplitude, assuming the longitudinal distribution of the current in the shower I in the correspondence with the cascade function to be very similar to the current distribution in the half-wave vibrator, i.e. when at the beginning and the end of path $I = 0$ (as on the vibrator's ends), and in the middle a maximum equal to

$$I_{\max} = 2I = 100 \text{ A}.$$

Then the field strength across the entire frequency range (see, for example, [46]) is

$$E = 60 \frac{I_{\max}}{R_{\text{me}}} = 0.75 \times 10^{-5} \text{ V m}^{-1},$$

and the spectral field component is $E_\omega = E/\Delta\omega = E\tau = 0.5$ μV m^{-1} MHz^{-1}. This crude estimate is very close to the field strength obtained in more consistent calculations (see above). Clearly, it is much smaller than the cosmic noise value.

There is a simple possibility of increasing the signal-to-noise ratio by several orders. For this a narrow-beamed antenna should be used. For example, the antenna of the radio telescope UTR-2 (Kharkov) has an effective area of $A = 10^5$ m^2 in the wavelength range 30-32 MHz. The angular size of the major lobe of the directivity diagram is less than 0.5° and for a given mode can change the position by any angle within the limits ±70° from the vertical. All these parameters correspond almost completely to the task pursued.

Reaching the Earth's surface, an electromagnetic wave carries energy $I_s = \varepsilon_0 c\pi E_\omega^2/\tau$ through 1 m^2 per second per unit solid angle. With a given cosmic noise intensity $I_n = 3 \times 10^{-40} T\nu^2 \Delta\Omega$ (W m^{-2} Hz^{-1}) [18], we get the signal-to-noise ratio

$$\frac{I_s}{I_n} = \frac{\varepsilon_0 c E_\omega^2}{3 \times 10^{-40} T\nu^2 \tau \Delta\Omega} \approx 10^5,$$

where the equivalent temperature of the celestial sphere T changes depending on the sidereal time and for the frequency $\nu = 30$ MHz is 2×10^4 K on average, $\tau = 3 \times 10^{-8}$ s is the emission process duration, and $\Delta\Omega = 0.8 \times 10^{-4}$ ster is the solid angle subtended by the major lobe of the radio telescope antenna directivity diagram. This estimate wittingly guarantees that the signal will be much stronger than the radio noise.

No master-signal to synchronize the registration technique is necessary in such an experiment. As it is absent for clear reasons, this means that special attention in this experiment should be given to protect the experimental set-up from noise. At frequencies above 30 MHz the ionosphere is known to be virtually transparent at night, especially in winter. So there is no disturbing influence of remote lightning discharges. So it remains to make allowance for radio noises caused by local thunderstorms and industrial noise. Local thunderstorms are dangerous only at distances above 150–200 km, as at frequencies $\nu \sim 30$ MHz the diffraction of waves on the curved surface of the Earth is insignificant. There are no thunderstorms in winter so it is the most favorable season for observations. It should also be noted that a lightning discharge can always be distinguished by the form of the signal which consists of intermittent pulses with a duration of hundreds of microseconds. There is another way of screening such noise, which we describe below.

The most dangerous is industrial noise. An arbitrary current short generates an electromagnetic field inducing an electric pulse in the surrounding conductors, which propagates along the wires as an electromagnetic wave along feeder lines. There are two ways the noise can penetrate into the registration block: 1) from the electromagnetic induction in the antenna's circuits and first amplification cascades, 2) directly from the industrial power supply of the experimental setup through power circuits and further on the first amplification cascades.

To block the noise from penetrating through the radio telescope antenna, a separate radio receiver with an unbeamed auxiliary antenna generates a pulse that blocks the input in the registration unit. In a similar way, the pulse passed through power circuits into preampilfication cascades can be blocked. For this, the noise signal comes to the input of a separate amplifier from the AC power supply through a small capacitor (such that $RC \sim 10^{-6}$ s). A top-hat pulse formed at its output blocks the registration channel. For the effective functioning of both protection systems, the signals induced in the radio telescope antenna are directed to the radio receiver through a delay line ($\sim 10^{-6}$ s).

Figure 8 [133] shows the block-scheme of one of the experimental set-ups tested in natural conditions. The antenna A_1 of the radio telescope (RI NANU UTR-2, Kharkov) is attached to the 6-unit band-filter BF ($\nu = 30$ MHz, $\Delta\nu = 2$ MHz). The signal amplified in the *HFA* cascade is detected and the high-frequency signal envelope is directed to the amplifier *IA*. The signal is retarded by the element *DL* by several microseconds and then passes to the input of the electronic key *EK* controlled by the formed top-hat pulse of regulated duration. It can be generated by an electromagnetic induction on the antenna A_2 or by the pulse that came from the AC power supply.

From this experiment the following information can be extracted:

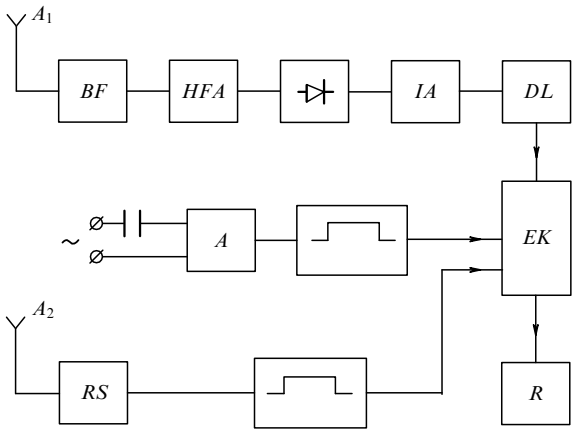

Figure 8. Block-scheme of the experimental set-up for detection of a radio pulse from a cosmic particle cascade on the Moon's surface.

a) an estimate of the flux intensity of cosmic rays with $W_0 = 10^{23}$ eV;

b) the directions for the calculation correction of the radiation field strength produced by the shower δ-electrons (for example, the account for the LPM effect);

c) some indication the anisotropy of cosmic rays with energy $W_0 = 10^{23}$ eV. For this it is necessary that the period of continuous observation be one year;

d) the grounds to prove the possibility (or impossibility) of realization of a radio detector in a near-lunar orbit.

This variant of testing the main points of the high-energy cosmic ray radio detection method is not unique. In [134] a scheme is proposed to carry out an experiment in the Antarctic Continent. The reason is that the majority of its surface is covered with ice to an altitude 3 – 4 km above sea level, which is the decisive factor. At these altitudes, an air shower reaches only the initial stage where the number of particles is almost an order of magnitude smaller than the maximum value. The main stage of the shower's development occurs at a depth of 10 – 15 m under the ice surface. The radio emission associated with the cascade process has almost the same power as in the case considered above, i.e. for the Moon. However, it is impossible to register the signal at distances above 10 – 20 km due to the finite curvature radius of the terrestrial surface. Nearly half of the energy emitted will reach the ionosphere and will be reflected backward, since the spectral intensity maximum in this case lies in the decameter wavelength range (50 – 100 m) and hence is below the maximum applicable frequency [111].

For example, one can imagine several posts with simple antennas and radio receivers located at a significant distance from each other on a continental area. They must be connected with the main registration center (having a simple computer for data analysis), for example by a satellite radio connection. In such an experiment, the expected radio signal can be selected by some specific properties. The above estimates suggest a field strength of about 1 $\mu V\ m^{-1}\ MHz^{-1}$ at a distance of 1000 km from the source. This is more than enough for the energy range available for studies to start from $W_0 = 10^{22}$ eV.

6. Conclusion

Numerous studies of the origin of radio emission associated with broad air showers in the meter wavelength range have definitely shown that the development of the radio detection method using the Cherenkov or geomagnetic radiation components holds little promise. For natural reasons, the direction of searches shifted toward long wavelengths. The subsequent discovery of the energy spectrum increase at low frequencies (< 1 MHz) stimulated the intensity of studies. However, nothing definite can be said about the nature of this phenomenon yet. Moreover, as this review shows, there are papers where this effect is not detected. So one can conclude that if there is a mechanism increasing the low-frequency radiation intensity, it should be more effective in denser media. This is likely one of the reasons for the increased interest in studying radio emission from cascade showers in dense media.

This far from complete review of studies of radio emission associated with cascade showers from high-energy cosmic particles shows that at present there is a sufficient quantity of facts (mainly theoretical) to continue the attempts at experimental justification of the possibility of cosmic ray detection using the radio component of the electromagnetic cascade emission. As the brief analysis of papers published over the last 10 – 15 years indicates, cascade phenomena in condensed media have become the preferred technique of theoretical studies. These include the lunar surface, the Antarctic ice cover, dielectric layers of natural dry sands, rock-salt, etc.

The set up of such experiments will differ substantially from traditional ones. These changes directly follow from the impossibility of using the master-signal for synchronization of the registering devices starting from the moment the cascade begins. So such experimental installations would require careful protection from atmospheric and industrial noise, as well as special programs for signal recognition. As was mentioned earlier [133], the first attempt to register cosmic rays using the radio telescope UTR-2 was greatly hampered by industrial noise where the rms amplitude was 1.5 to 2 orders of magnitude higher than the cosmic noise amplitude. The effective system for industrial noise suppression described above decreased the false event rate by three to four orders, however this proved insufficient for the experiment to continue. So the idea of mounting a radio detector onboard a lunar orbiting spacecraft, discussed in many papers, is fruitful in many respects. It is likely that this method will be studied most actively in the near future.

References

1. Hayashida N et al. *Phys. Rev. Lett.* **77** 1000 (1996)
2. Mikhaĭlov A A *Izv. Ross. Akad. Nauk Ser. Fiz.* **63** 556 (1999)
3. Khristiansen G B et al. *Izv. Akad. Nauk SSSR Ser. Fiz.* **53** 286 (1989)
4. Atrashkevich V B et al. *Izv. Ross. Akad. Nauk Ser. Fiz.* **63** 534 (1999)
5. Schwarzschild B *Phys. Today* **50** (2) 19 (1997)
6. Askar'yan G A *Zh. Eksp. Teor. Fiz.* **41** 616 (1961) [*Sov. Phys. JETP* **14** 441 (1962)]
7. Kahn F D, Lerche I *Proc. R. Soc. London Ser. A* **289** 206 (1966)
8. Ginzburg V L *Teoreticheskaya Fizika i Astrofizika* (Theoretical Physics and Astrophysics) 2nd ed. (Moscow: Nauka, 1981) [Translated into English: *Applications of Electrodynamics in Theoretical Physics and Astrophysics* (New York: Gordon and Breach Sci. Publ., 1989)]
9. Filonenko A D *Zh. Tekh. Fiz.* **71** (3) 88 (2001) [*Phys. Tech. Phys.* **46** 357 (2001)]
10. Golubnichiĭ P I, Filonenko A D *Pis'ma Zh. Tekh. Fiz.* **20** (12) 57 (1994) [*Tech. Phys. Lett.* **20** 499 (1994)]
11. Golubnichiĭ P I, Filonenko A D, Yakovlev V I *Izv. Ross. Akad. Nauk Ser. Fiz.* **58** (12) 115 (1994)
12. Golubnichiĭ P I, Filonenko A D *Ukr. Fiz. Zh.* **41** 696 (1996)
13. Filonenko A D *Izv. Ross. Akad. Nauk Ser. Fiz.* **61** 543 (1997)
14. Filonenko A D *Pis'ma Zh. Eksp. Teor. Fiz.* **70** 639 (1999) [*JETP Lett.* **70** 649 (1999)]
15. Filonenko A D *Pis'ma Zh. Tekh. Fiz.* **23** (10) 57 (1997) [*Tech. Phys. Lett.* **23** 399 (1997)]
16. Akhiezer A I *Atomnaya Fizika.* Spravochnoe Posobie (Handbook on Atomic Physics) (Kiev: Naukova Dumka, 1988)
17. Murzin V S *Vvedenie v Fiziku Kosmicheskikh Lucheĭ* (Introduction to Cosmic Ray Physics) (Moscow: Izd. MGU, 1988)
18. Kikoin I K (Ed.) *Tablitsy Fizicheskikh Velichin* (Tables of Physical Quantities) (Moscow: Atomizdat, 1976)
19. Askar'yan G A *Zh. Eksp. Teor. Fiz.* **48** 988 (1965) [*Sov. Phys. JETP* **21** 658 (1965)]
20. Levich V G *Kurs Teoreticheskoĭ Fiziki* (Course of Theoretical Physics) 2nd ed. Vol. 1 (Moscow: Nauka, 1969) [Translated into English: *Theoretical Physics. An Advanced Text* Vol. 1, 2 (Amsterdam: North-Holland Publ. Co., 1971)]
21. Charman W N *Nature* **215** 497 (1967)
22. Charman W N, Jelley J V *Can. J. Phys.* **46** 216 (1968)
23. Sivaprasad K, in *15th Cosmic Ray Conf., Plovdiv, Bulgaria, 1977: Conf. Papers* (Eds C Ya Christov et al.) Vol. 8 (Sofia: Institute for Nucl. Res. and Nucl. Energy, Bulgarian Acad. of Sci., 1978) p. 484
24. Tompkins D R (Jr) *Phys. Rev. D* **10** 136 (1974)

25. Sivaprasad K *Aust. J. Phys.* **31** 439 (1978)
26. Suga K, Nishi K, in *20th Intern. Cosmic Ray Conf., Moscow, USSR, 1987: Conf. Papers* (Eds V A Kozyarivsky et al.) Vol. 6 (Moscow: Nauka, 1987) p. 125
27. Kusunose M, Sasaki H, Ogawa T, in *22nd Intern. Cosmic Ray Conf., Dublin, Ireland, 1991: Conf. Papers* (Eds M Cawley et al.) Vol. 4 (Dublin: The Dublin Inst. for Adv. Studies, 1991) p. 359
28. Aleksandrov A V et al., in *20th Intern. Cosmic Ray Conf., Moscow, USSR, 1987: Conf. Papers* (Eds V A Kozyarivsky et al.) Vol. 6 (Moscow: Nauka, 1987) p. 132
29. Filonenko A D *Pis'ma Zh. Tekh. Fiz.* **27** (10) 9 (2001) [*Tech. Phys. Lett.* **27** 398 (2001)]
30. Landau L D, Lifshitz E M *Teoriya Polya* (The Classical Theory of Fields) (Moscow: Nauka, 1967) [Translated into English (Oxford: Pergamon Press, 1971)]
31. Raĭzer Yu P *Fizika Gazovogo Razryada* (Gas Discharge Physics) (Moscow: Nauka, 1987) [Translated into English (Berlin: Springer-Verlag, 1991)]
32. Rozental' I L, Fil'chenkov M L *Izv. Akad. Nauk SSSR Ser. Fiz.* **30** 1703 (1966)
33. Jelley J V *Phys. Lett. A* **25** 346 (1967)
34. Belen'kiĭ S Z *Lavinnye Protsessy v Kosmicheskikh Luchakh* (Avalanche Processes in Cosmic Rays) (Moscow: GITTL, 1948)
35. Volovik V D, Zalyubovskiĭ I I, Shmatko E S *Izv. Akad. Nauk SSSR Ser. Fiz.* **40** 1026 (1976)
36. Filonenko A D *Zh. Tekh. Fiz.* **70** (10) 132 (2000) [*Phys. Tech. Phys.* **45** 1362 (2000)]
37. Bagrov V G, Ternov I M, Fedosov N I *Zh. Eksp. Teor. Fiz.* **82** 1442 (1982) [*Sov. Phys. JETP* **55** 835 (1982)]
38. Nishimura J, in *19th Intern. Cosmic Ray Conf., La Jolla, USA, 1985: Conf. Papers* (NASA Conf. Publ., № 2376, Eds F C Jones et al.) Vol. 7 (Washington, D.C.: Sci. and Tech. Inform. Branch, NASA, 1985) p. 308
39. Baishya R et al., in *25th Intern. Cosmic Ray Conf., Durban, South Africa, 1997: Conf. Papers* (Eds M S Potgieter et al.) Vol. 6 (Wesprint: Potchefstroom Univ., Space Res. Unit, 1997) p. 237
40. Datta P, Pathak K M, in *21st Intern. Cosmic Ray Conf., Adelaide, Australia, 1990: Conf. Papers* (Ed. R J Protheroe) Vol. 9 (Northfield: Department of Phys. and Math. Phys., The Univ. of Adelaide, Graphic Services, 1990) p. 218
41. Filonenko A D *Izv. Ross. Akad. Nauk Ser. Fiz.* **63** 565 (1999)
42. Filonenko A D *Zh. Tekh. Fiz.* **70** (10) 127 (2000) [*Phys. Tech. Phys.* **45** 1357 (2000)]
43. Kulikovskiĭ A N (Ed.) *Spravochnik po Teoreticheskim Osnovam Radioelektroniki* (Handbook on Theoretical Grounds of Radioelectronics) Vol. 1 (Moscow: Energiya, 1977)
44. Bobrov N V (Ed.) *Radiopriemnye Ustroĭstva* (Radio Receivers) (Moscow: Sov. Radio, 1971)
45. Ginzburg V L *Usp. Fiz. Nauk* **166** 169 (1996) [*Phys. Usp.* **39** 155 (1996)]
46. Pistol'kors A A *Antenny* (Antennae) (Moscow: Svyaz'izdat, 1947)
47. Golubnichiĭ P I, Filonenko A D, Tsarev V A *Izv. Akad. Nauk SSSR Ser. Fiz.* **55** 727 (1991)
48. Golubnichiĭ P I, Filonenko A D *Izv. Akad. Nauk SSSR Ser. Fiz.* **53** 366 (1989)
49. McDonald D M, Prescott J R, in *17th Intern. Cosmic Ray Conf., Paris, France, 1981: Conf. Papers* Vol. 6 (Gif-sur-Yvette: Sect. d'Astrophys., Service de Documentation du CEN de Saclay, 1981) p. 82
50. Gusev G A, Zheleznykh I M *Pis'ma Zh. Eksp. Teor. Fiz.* **38** 505 (1983) [*JETP Lett.* **38** 611 (1983)]
51. Jelley J V et al. *Nature* **205** 327 (1965)
52. Jelley J H et al. *Nuovo Cimento A* **46** 649 (1966)
53. Borzhkovskiĭ I A, Volovik V D, Shmatko E S *Izv. Akad. Nauk SSSR Ser. Fiz.* **30** 1705 (1966)
54. Borzhkovskiĭ I A et al. *Pis'ma Zh. Eksp. Teor. Fiz.* **3** (4) 186 (1966) [*JETP Lett.* **3** 126 (1966)]
55. Vernov S N et al. *Pis'ma Zh. Eksp. Teor. Fiz.* **5** 157 (1967) [*JETP Lett.* **5** 126 (1967)]
56. Vernov S N et al. *Izv. Akad. Nauk SSSR Ser. Fiz.* **32** 467 (1968)
57. Vernov S N et al. *Izv. Akad. Nauk SSSR Ser. Fiz.* **34** 1995 (1970)
58. Khristiansen G B et al. *Izv. Akad. Nauk SSSR Ser. Fiz.* **35** 2102 (1971)
59. Atrashkevich V B, Vedeneev O V, Khristiansen G B *Pis'ma Zh. Eksp. Teor. Fiz.* **13** (1) 76 (1971) [*JETP Lett.* **13** 53 (1971)]
60. Atrashkevich V B et al. *Izv. Akad. Nauk SSSR Ser. Fiz.* **36** 1731 (1972)
61. Vernov S N et al. *Izv. Akad. Nauk SSSR Ser. Fiz.* **28** 2087 (1964)
62. Volovik V D et al. *Izv. Akad. Nauk SSSR Ser. Fiz.* **38** 1013 (1974)
63. Allan H R et al., in *12th Intern. Conf. on Cosmic Rays, Hobart, Australia, 1971: Papers* (Eds A G Fenton, K B Fenton) Vol. 3 (Hobart: Univ. of Tasmania Press, 1971) p. 1097
64. Allan H R et al., in *12th Intern. Conf. on Cosmic Rays, Hobart, Australia, 1971: Papers* (Eds A G Fenton, K B Fenton) Vol. 3 (Hobart: Univ. of Tasmania Press, 1971) p. 1102
65. Volovik V D, Zalyubovskiĭ I I, Shmatko E S *Izv. Akad. Nauk SSSR Ser. Fiz.* **40** 1026 (1976)
66. Beĭsembaev R U, Vavilov Yu N, Volovik V D *Kratk. Soobshch. Fiz.* (1) 9 (1980)
67. Allan H R, Jones J K *Nature* **212** 129 (1966)
68. Allan H R et al. *Nature* **222** 635 (1969)
69. Allan H R, Neat K P, Jones J K *Nature* **215** 267 (1967)
70. Allan H R, Clay R W, Jones J K *Nature* **227** 1116 (1970)
71. Allan H R, Clay R W, Jones J K *Nature* **225** 253 (1970)
72. Allan H R *Acta Phys. Hung.* **29** (Suppl. 3) 699 (1970)
73. Allan H R, in *12th Intern. Conf. on Cosmic Rays, Hobart, Australia, 1971: Papers* (Eds A G Fenton, K B Fenton) Vol. 3 (Hobart: Univ. of Tasmania Press, 1971) p. 1113
74. Allan H R, in *Progress in Elementary Particles and Cosmic Ray Physics* Vol. 10 (Eds J G Wilson, S G Wouthuysen) (Amsterdam: North-Holland, 1971) p. 171
75. Allan H R, Shutie P F, Sun M P, in *13th Intern. Cosmic Ray Conf., Denver, Colorado, USA, 1973: Conf. Papers* (Ed. R L Chasson) Vol. 4 (Boulder, C.O.: Colorado Associated Univ. Press, 1973) p. 2407
76. Allan H R, Sun M P, Jones J K, in *14th Intern. Cosmic Ray Conf., München, FRG, 1975: Conf. Papers* (Ed. K Pinkau) Vol. 8 (München: Max-Planck-Institut für Extraterrestrische Physik, 1975) p. 3082
77. Allan H R et al., in *14th Intern. Cosmic Ray Conf., München, FRG, 1975: Conf. Papers* (Ed. K Pinkau) Vol. 8 (München: Max-Planck-Institut für Extraterrestrische Physik, 1975) p. 3077
78. Pathak K M, Barthakur S K, in *15th Intern. Cosmic Ray Conf., Plovdiv, Bulgaria, 1977: Conf. Papers* (Eds C Ya Christov et al.) Vol. 8 (Sofia: Inst. for Nucl. Res. and Nucl. Energy, Bulgarian Acad. of Sci., 1978) p. 541
79. Goswami D C, Pathak K M *Nuovo Cimento B* **39** 55 (1977)
80. Goswami D C, Pathak K M *Nuovo Cimento B* **39** 65 (1977)
81. Barthakur S K, Barua P K, Pathak K M, in *16th Intern. Cosmic Ray Conf., Kyoto, Japan, 1979: Conf. Papers* (Ed. S Miyake) Vol. 9 (Tokyo: Inst. of Cosmic Ray Res., Univ. of Tokyo Press, 1980) p. 26
82. Barthakur S K, Barua P K, Pathak K M, in *16th Intern. Cosmic Ray Conf., Kyoto, Japan, 1979: Conf. Papers* (Ed. S Miyake) Vol. 9 (Tokyo: Inst. of Cosmic Ray Res., Univ. of Tokyo Press, 1980) p. 31
83. Barthakur S K et al., in *16th Intern. Cosmic Ray Conf., Kyoto, Japan, 1979: Conf. Papers* (Ed. S Miyake) Vol. 9 (Tokyo: Inst. of Cosmic Ray Res., Univ. of Tokyo Press, 1980) p. 36
84. Barthakur S K, Barua P K, Pathak K M *Indian. J. Pure Appl. Phys.* **17** 598 (1979)
85. Barthakur S K, Barua P K, Pathak K M *Indian. J. Pure Appl. Phys.* **19** 388 (1981)
86. Barthakur S K, Barua P K, Pathak K M *Indian. J. Pure Appl. Phys.* **17** 601 (1979)
87. Borah B, Datta P, Pathak K M, in *18th Intern. Cosmic Ray Conf., Bangalore, India, 1983: Papers and Proc.* (Eds N Durgaprasad et al.) Vol. 6 (Bombay: Tata Inst. of Fundamental Res., 1983) p. 245
88. Borah B, Datta P, Pathak K M, in *18th Intern. Cosmic Ray Conf., Bangalore, India, 1983: Papers and Proc.* (Eds N Durgaprasad et al.) Vol. 6 (Bombay: Tata Inst. of Fundamental Res., 1983) p. 253
89. Pathak K M et al., in *17th Intern. Cosmic Ray Conf., Paris, France, 1981: Conf. Papers* Vol. 6 (Gif-sur-Yvette: Sect. d'Astrophys., Service de Documentation du CEN de Saclay, 1981) p. 86
90. Borah B, Datta P, Pathak K M *Indian. J. Pure Appl. Phys. B* **57** 267 (1983)
91. Borah B, in *18th Intern. Cosmic Ray Conf., Bangalore, India, 1983: Papers and Proc.* (Eds N Durgaprasad et al.) Vol. 6 (Bombay: Tata Inst. of Fundamental Res., 1983) p. 249

92. Datta P, Pathak K M, in *19th Intern. Cosmic Ray Conf., La Jolla, USA, 1985: Conf. Papers* (NASA Conf. Publ., № 2376, Eds F C Jones et al.) Vol. 7 (Washington, D.C.: Sci. and Tech. Inform. Branch, NASA, 1985) p. 272
93. Pathak K M, Mazumdar G K D, in *19th Intern. Cosmic Ray Conf., La Jolla, USA, 1985: Conf. Papers* (NASA Conf. Publ., № 2376, Eds F C Jones et al.) Vol. 7 (Washington, D.C.: Sci. and Tech. Inform. Branch, NASA, 1985) p. 276
94. Datta P, Pathak K M, in *20th Intern. Cosmic Ray Conf., Moscow, USSR, 1987: Conf. Papers* (Eds V A Kozyarivsky et al.) Vol. 6 (Moscow: Nauka, 1987) p. 129
95. Prescott J R et al. *Can. J. Phys.* **46** 246 (1968)
96. Clay R W et al., in *14th Intern. Cosmic Ray Conf., München, FRG, 1975: Conf. Papers* (Ed. K Pinkau) Vol. 8 (München: Max-Planck-Institut für Extraterrestrische Physik, 1975) p. 3093
97. Hazen W E et al. *Phys. Rev. Lett.* **22** 35 (1969)
98. Hazen W E et al. *Phys. Rev. Lett.* **24** 476 (1970)
99. Atrashkevich V B, Khristiansen G B, in *17th Intern. Cosmic Ray Conf., Paris, France, 1981: Conf. Papers* Vol. 6 (Gif-sur-Yvette: Sect. d'Astrophys., Service de Documentation du CEN de Saclay, 1981) p. 318
100. Bagio R et al. *Nuovo Cimento B* **40** 289 (1977)
101. Atrashkevish V B et al. *Yad. Fiz.* **28** 712 (1978)
102. Atrashkevich V B, Vedeneev O V, Khristiansen G B, in *14th Intern. Cosmic Ray Conf., München, FRG, 1975: Conf. Papers* (Ed. K Pinkau) Vol. 8 (München: Max-Planck-Institut für Extraterrestrische Physik, 1975) p. 3086
103. Mandolesi N, Morigi G, Palumbo G G C *J. Atmos. Terr. Phys.* **36** 1431 (1974)
104. Mandolesi N, Morigi G, Palumbo G G, in *13th Intern. Cosmic Ray Conf., Denver, Colorado, USA, 1973: Conf. Papers* (Ed. R L Chasson) Vol. 4 (Boulder, C.O.: Colorado Associated Univ. Press, 1973) p. 2414
105. Mandolesi N, Morigi G, Palumbo G G C *J. Phys. A* **9** 815 (1976)
106. Prescott J R, Hough J H, Pidcock J K *Acta Phys. Hung.* **29** (Suppl. 3) 717 (1970)
107. Stubbs T J *Nature* **230** 172 (1971)
108. Hough J H, Prescott J R, Clay R W *Nature* **232** 14 (1971)
109. Allan H R *Nature* **237** 384 (1972)
110. Colgate S A *J. Geophys. Res.* **72** 4869 (1967)
111. Dolukhanov M P *Rasprostranenie Radiovoln* (Propagation of Radio Waves) (Moscow: Svyaz', 1972) [Translated into English (Moscow: Mir Publ., 1971)]
112. Felgate D G, Stubbs T J *Nature* **239** 151 (1972)
113. Kaneko T et al., in *18th Intern. Cosmic Ray Conf., Bangalore, India, 1983: Papers and Proc.* (Eds N Durgaprasad et al.) Vol. 11 (Bombay: Tata Inst. of Fundamentals Res., 1983) p. 428
114. Frank I M *Izluchenie Vavilova – Cherenkova: Voprosy Teorii* (Vavilov – Cherenkov Radiation: Questions of Theory) (Moscow: Nauka, 1988)
115. Datta P et al., in *22nd Intern. Cosmic Ray Conf., Dublin, Ireland, 1991: Conf. Papers* (Eds M Cawley et al.) Vol. 4 (Dublin: The Dublin Inst. for Adv. Studies, 1991) p. 371
116. Clay R W et al., in *13th Intern. Cosmic Ray Conf., Denver, Colorado, USA, 1973: Conf. Papers* (Ed. R L Chasson) Vol. 4 (Boulder, C.O.: Colorado Associated Univ. Press, 1973) p. 2420
117. Suga K, Kakimoto F, Nishi K, in *19th Intern. Cosmic Ray Conf., La Jolla, USA, 1985: Conf. Papers* (NASA Conf. Publ., № 2376, Eds F C Jones et al.) Vol. 7 (Washington, D.C.: Sci. and Tech. Inform. Branch, NASA, 1985) p. 268
118. Kaneko T, Suga K, in *18th Intern. Cosmic Ray Conf., Bangalore, India, 1983: Papers and Proc.* (Eds N Durgaprasad et al.) Vol. 11 (Bombay: Tata Inst. of Fundamental Res., 1983) p. 428
119. Honda K et al., in *22nd Intern. Cosmic Ray Conf., Dublin, Ireland, 1991: Conf. Papers* (Eds M Cawley et al.) Vol. 4 (Dublin: The Dublin Inst. for Adv. Studies, 1991) p. 367
120. Belyaev A A et al. *Elektronno-fotonnye Kaskady v Kosmicheskikh Luchakh pri Sverkhvysokikh Energiyakh* (Electron-Photon Cascades from Super-high Energy Cosmic Rays) (Ed. Ambrosimov A T) (Moscow: Nauka, 1980)
121. Kakimoto F et al., in *21st Intern. Cosmic Ray Conf., Adelaide, Australia, 1990: Conf. Papers* (Ed. R J Protheroe) Vol. 9 (Northfield: Department of Phys. and Math. Phys., The Univ. of Adelaide, Graphic Services, 1990) p. 213
122. Raĭzer Yu P *Osnovy Sovremennoĭ Fiziki Gazorazryadnykh Protsessov* (Grounds of Modern Physics of Gas Discharge Processes) (Moscow: Nauka, 1980)
123. Abramowitz M, Stegun I A (Eds) *Handbook on Mathematical Functions, with Formulas, Graphs and Mathematical Tables* (New York: Dover Publ., 1965) [Translated into Russian (Moscow: Nauka, 1979)]
124. Kadota et al., in *23rd Intern. Cosmic Ray Conf., Calgary, Canada, 1993: Conf. Papers* (Ed. D A Leahy) Vol. 4 (Calgary: Department of Phys. and Astron., The Univ. of Calgary, 1993) p. 262
125. Askar'yan G A *Pis'ma Zh. Eksp. Teor. Fiz.* **39** 334 (1984) [*JETP Lett.* **39** 402 (1984)]
126. Dagkesamanskiĭ R D, Zheleznykh I M *Pis'ma Zh. Eksp. Teor. Fiz.* **50** 233 (1989) [*JETP Lett.* **50** 259 (1989)]
127. Berezinskiĭ V S, Gazizov A Z *Pis'ma Zh. Eksp. Teor. Fiz.* **25** 276 (1977) [*JETP Lett.* **25** 254 (1977)]
128. Alvarez-Muniz J, Zas E, in *25th Intern. Cosmic Ray Conf., Durban, South Africa, 1997: Conf. Papers* (Eds M S Potgier et al.) Vol. 7 (Wesprint: Potchefstroom Univ., Space Res. Unit, 1997) p. 309
129. Dedenko L G, Kolomatskiĭ S G *Izv. Akad. Nauk SSSR Ser. Fiz.* **53** 321 (1989)
130. Dedenko L G et al. *Izv. Ross. Akad. Nauk Ser. Fiz.* **63** 589 (1999)
131. Golubnichiĭ P I, Filonenko A D *Kosmich. Nauka Tekhnol.* **5** (4) 87 (1999)
132. Filonenko A D *Pis'ma Zh. Tekh. Fiz.* **28** (3) 60 (2002) [*Tech. Phys. Lett.* **28** 110 (2002)]
133. Abranin E P et al. *Izv. Ross. Akad. Nauk Ser. Fiz.* **65** 1970 (2001)
134. Filonenko A D *Pis'ma Zh. Tekh. Fiz.* **24** (24) 65 (1998) [*Tech. Phys. Lett.* **24** 975 (1998)]